vol. 47, n.° 3, septiembre-diciembre de 2025
ISSN impreso: 0120-0283 • ISSN en línea: 2145-8553

Provenance of Lower Eocene strata of the San Jacinto Fold Belt (Colombian Caribbean): paleogeographic, and magmatic implications

Ángel Antonio Barbosa-Espitia[1,2]*; Andrés Pardo-Trujillo[2]; David Foster[3]

[1] Dirección Académica, Universidad Nacional de Colombia, La Paz, Colombia.
(*) abarbosae@unal.edu.co
[2] Instituto de Investigaciones en Estratigrafía, Universidad de Caldas, Manizales, Colombia.
andres.pardo@ucaldas.edu.co
[3] Department of Geological Sciences, University of Florida, Gainesville, USA. dafoster@ufl.edu

Abstract

The Eocene infill of the San Jacinto Fold Belt (SJFB) contains information of the paleogeographic and magmatic evolution of the northwesternmost corner of the Andes. This information is clue to find prospective rocks for hydrocarbons and CO_2 storage reservoirs. In this study, we report new sandstone petrography and detrital zircon U-Pb geochronology analyses from three Lower Eocene boreholes drilled at two locations in the SJFB in order to investigate the provenance, paleogeography and magmatic contribution to the basin. The combined provenance analysis reveals multiple sources of detritus, including arc-like igneous, metamorphic and sedimentary rocks with two main U-Pb age populations (Cretaceous-Paleogene and Permian-Triassic). These ages and composition of the detritus are consistent with rock sources in the basement of the Lower Magdalena Valley (LMV) and the Central Cordillera (CC), transported to the SJFB by a short-distance drainage network. Eocene zircons found in the studied rocks suggest that arc magmatism was locally active with sources located at the Sierra Nevada de Santa Marta (SNSM) or nearby. Furthermore, vertical and geographic variability of sandstones compositional maturity in the studied wells seem to be controlled by the depositional paleoenvironment, being the sandstones from the deeper northern part of the basin more mature (less proportion of lithics in the QFL diagram) than their shallower southern counterpart.

Keywords: Caribbean basins; Lower Magdalena Basin; Paleogeography; Northern Andes; Provenance; Magmatism.

Proveniencia de los estratos Eoceno Inferior del cinturón plegado de San Jacinto (Caribe colombiano): implicaciones paleogeográficas y magmáticas

Resumen

El relleno Eoceno del cinturón plegado de San Jacinto (CPSJ) contiene información de la paleogeografía y evolución magmática de la esquina más noroccidental de los Andes. Esta información es vital para encontrar rocas prospectivas para almacenamiento de hidrocarburos o reservorios de CO_2. En este estudio reportamos nuevos análisis de petrografía de areniscas y geocronología U-Pb en circones detríticos de tres pozos Eoceno Inferior perforados en dos localidades del CPSJ con el fin de investigar la proveniencia, paleogeografía, y contribución magmática a la cuenca. El análisis

How to cite: Barbosa-Espitia, Á.A.; Pardo-Trujillo, A.; Foster, D.A. (2025). Provenance of Lower Eocene strata of the San Jacinto Fold Belt (Colombian Caribbean): paleogeographic, and magmatic implications. *Boletín de Geología, 47*(3), 13-38. https://doi.org/10.18273/revbol.v47n3-2025001

combinado de proveniencia revela múltiples fuentes de detríticos, incluidas rocas ígneas de arco, rocas metamórficas y rocas sedimentarias, con dos poblaciones principales de edades U-Pb (Cretácico-Paleoceno y Pérmico-Triásico). Estas edades y composición detrítica son consistentes con fuentes de rocas en el basamento de la cuenca del Valle Inferior del Magdalena (VIM) y la cordillera Central (CC), trasportadas al CPSJ por una red de drenajes de corta distancia. Los circones Eocenos encontrados en las rocas estudiadas sugieren que el magmatismo de arco estuvo activo localmente con fuentes localizadas en la Sierra Nevada de Santa Marta (SNSM) o cercanas. Además, la variabilidad vertical y geográfica en la madurez composicional de las areniscas en los pozos estudiados parece estar controlada por el paleoambiente de depósito, siendo las areniscas de la parte norte y más profunda de la cuenca más maduras (menos proporción de líticos en el diagrama QFL) comparadas con las areniscas de la parte sur.

Palabras clave: Cuencas del caribe; Cuenca del Valle Inferior del Magdalena; Paleogeografía; Andes del norte; Proveniencia; Magmatismo.

Introduction

The northern Andes of Colombia are a complex geologic region characterized by the interaction of the Caribbean Plate with the South American continental margin (Figure 1). This interaction began during the Cretaceous and continued through the Cenozoic (Cediel *et al*., 2003; Kennan and Pindell, 2009; Pindell and Kennan, 2009; Villagómez *et al*., 2011a; Villagómez and Spikings, 2013). The Eocene in the Colombian Caribbean region was characterized by an increase in morphotectonic activity (Cardona *et al*., 2011a; Villagómez *et al*., 2011b; Parra *et al*., 2020). One of the Caribbean regions that developed and deformed during this activity is the San Jacinto Fold Belt (SJFB), a SW-NE trending tectonic province located near to the northern end of the western South American convergent margin (Figure 1). Eocene strata in the SJFB outcrop along the Colombian margin and record important information about the tectonics, paleogeography and magmatic evolution of the northern Andes (e.g., Cardona *et al*., 2012; Silva-Arias *et al*., 2016; Osorio-Granada *et al*., 2020). Additionally, some of these units have been studied for their high potential as hydrocarbon reservoirs (e.g., Barrero *et al*., 2007) and indeed the only commercial hydrocarbon field in the whole SJFB produces gas from middle Eocene reservoirs (Sierra *et al*., 2024). Previous studies on Eocene sequences have been useful to understand local distribution of the sequence. These studies although valuable, need to be complemented with additional studies in other portions of the basin to gain a better understanding of the petrographic and provenance characteristics of the Lower Eocene sequence. Furthermore, there is not currently a paleogeographic reconstruction for the Ypresian in the SJFB that can be used for understanding the spatial distribution of potential reservoir rocks and the continuity of the Paleogene magmatic arc reported in the CC and the SNSM (e.g., Cardona *et al*., 2018).

In this paper, we present new petrography and detrital zircon U-Pb data from three drilled holes, two located northward SJFB (ANH-Piedras Blancas-1X, ANH-San Cayetano-1) and one located ~150 km southward (ANH-La X-1A), along with previously reported petrographic and geochronologic data for the Lower Eocene sedimentary rocks from other wells or outcrops in the SJFB to define the provenance of the Lower Eocene sedimentary infill of the SJFB and thus constrain the Lower Eocene paleogeography of the Colombian Caribbean region and the contribution of arc magmatism to the SJFB. The results of these analyses increase our understanding of the geology and petroleum systems in the Colombian Caribbean basins during Lower Eocene and yield new data and interpretations for improving Cenozoic tectonic reconstructions of the northern Andes.

Geological Setting

The SJFB is a SW-NE trending tectonic province located close to the northern end of the western South American convergent margin. It is bounded to the east by the Romeral fault system, which separates it from the Lower Magdalena Valley (LMV). The Santa Marta-Bucaramanga fault system separates the northernmost SJFB from the Sierra Nevada de Santa Marta (SNSM), while the Sinú lineament separates the SJFB from the Sinú fold belt to the west (Duque-Caro, 1979, 1980; Camargo, 1995; Reyes and Camargo, 1995) (Figure 1). The structural evolution of the SJFB is related to the transpressional-

transtensional deformation caused by the relative displacement of the Caribbean Plate (Flinch, 2003; Guzmán, 2007; Mora-Bohórquez *et al*., 2020). The basement is composed of mafic volcanic rocks intruded by plutons interpreted as the continuation of a Cretaceous oceanic island arc developed over the Caribbean Plate and subsequently accreted along western Colombia (Cardona *et al*., 2012), or as an arc that developed *in situ* after the accretion of the oceanic terrain onto the continent (Mora *et al*., 2017; Mora-Bohórquez *et al*., 2020). Although this tectonic history has been adopted by many authors, the origin of the SJFB and its geographic extent are still hotly debated (e.g., Ardila and Diaz, 2015). The oldest sedimentary rocks in the study area are composed of marine deposits of the Cansona Formation (Campanian - Maastrichtian), which were unconformably deposited on the basement of oceanic affinity (Duque-Caro, 1979; Guzmán *et al*., 2004; Guzmán, 2007). After deposition of the Cansona Formation, an erosional/depositional gap between the Maastrichtian and Early Paleogene occurred, possibly due to the collision of the Caribbean Plateau against the northern South American margin (Cardona *et al*., 2012). Subsequently, a thick sequence of conglomerates, fluvial-deltaic sandstones and shallow marine mudstones with abundant mollusks of the San Cayetano Formation (Paleocene-early Eocene) was deposited (Figure 2). This sequence is unconformably overlain by middle Eocene deltaic deposits and platform carbonates of the Toluviejo and Arroyo de Piedra formations (Mora-Bohórquez *et al*., 2025; Patarroyo *et al*., 2025), though in some areas it is directly overlain by bioclastic limestones interbedded with fossiliferous calcareous sandstones; as well as mudstones of deltaic and shallow marine deposits of the late Eocene-Oligocene San Jacinto Formation (Guzmán *et al*., 2004; Guzmán, 2007; ANH-Universidad de Caldas, 2009). Sedimentation in the Oligocene-Miocene interval is characterized by thick successions of sandstones interbedded with mudstones and some coal beds of the Ciénaga de Oro Formation (Guzmán *et al*., 2004; Mora *et al*., 2018).

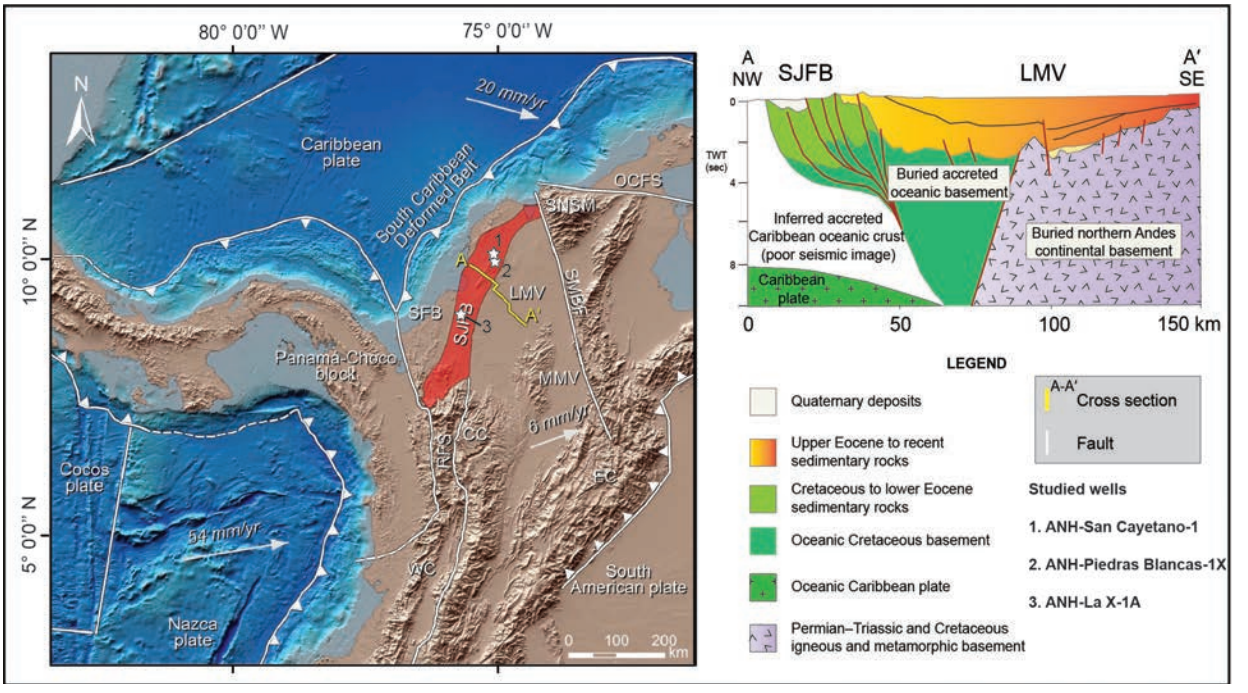

Figure 1. Geodynamic framework of northwestern South America showing the major Andean Mountain ranges, faults, crustal blocks, and surrounding tectonic plates. A-A' cross section shows the basement configuration and sedimentary basins of the northwestern margin of South America modified from Osorio-Granada *et al*. (2020). WC: Western Cordillera; CC: Central Cordillera; SJFB: San Jacinto Fold Belt; SFB: Sinu fold belt; LMV: Lower Magdalena Valley; MMV: Middle Magdalena Valley; RFS: Romeral Fault System; SMBF: Santa Marta-Bucaramanga fault system; OCFS: Oca fault system; SNSM: Sierra Nevada de Santa Marta.

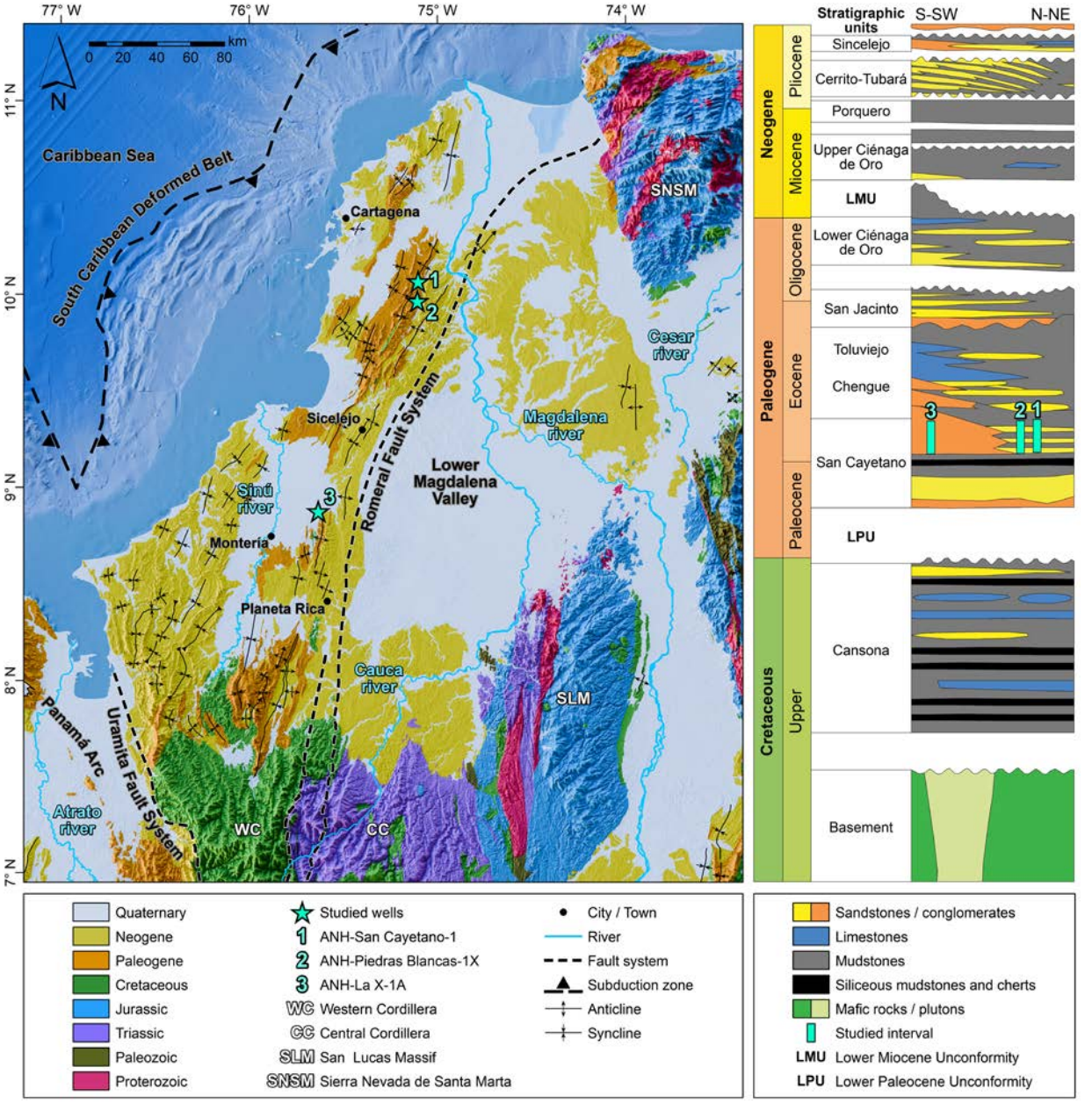

Figure 2. Geologic map of the northern most Andes showing the location of the studied wells, and litho and chronostratigraphy of the sedimentary sequences in the region. Lithology according to Piraquive *et al*. (2022) and Gómez *et al*. (2023), chrono and lithostratigraphy according to Mora-Bohórquez *et al*. (2017) and Mora *et al*. (2018).

Potential sediment sources from previous studies

Four main sources of sediments for the Eocene sedimentary sequences at the SJFB coming from surrounding areas are inferred from previous studies (e.g., Montes *et al*., 2010; Silva-Arias *et al*., 2016; Mora-Bohórquez *et al*., 2017) (Figure 2). These sources may be currently exposed or covered by sediments. The first rock source corresponds to Permo-Triassic metamorphic rocks (schists and phyllites) from the basement of the LMV and the CC (Vinasco *et al*., 2006; Montes *et al*., 2010; Villagómez *et al*., 2011a; Silva-Arias *et al*., 2016). The second rock source corresponds to Permo-Triassic felsic plutonic rocks from the basement of

the LMV (Montes *et al*., 2010; Silva-Arias *et al*., 2016). The third source corresponds to Cretaceous mafic to intermediate plutonic and volcanic rocks from the LMV basement and the CC (Villagómez *et al*., 2011a; Silva-Arias *et al*., 2016; Mora-Bohórquez *et al*., 2017). The fourth source corresponds to Late Cretaceous-Paleocene sedimentary rocks (mudstones, limestones and sandstones) from the SJFB (Cardona *et al*., 2012; Dueñas-Jiménez and Gómez-González, 2013; Angulo-Pardo *et al*., 2023). In addition, minor sources of sediments coming from more distant regions include Precambrian high grade metamorphic rocks (gneisses, migmatites, granulites), Jurassic intermediate plutonic and volcanic rocks from the San Lucas massif (SLM) and the SNSM; and Proterozoic (amphibolites to granulites) and Paleocene plutonic rocks from the SNSM (Ordóñez-Carmona *et al*., 2009; Cardona *et al*., 2010a, 2011a; Cochrane *et al*., 2014; Piraquive *et al*., 2022).

Stratigraphy of the studied wells

The Lower-Middle Eocene in the SJFB, corresponding to part of the San Cayetano Formation (Vallejo-Hincapié *et al*., 2023), was drilled in three core wells funded by the Colombian Hydrocarbons Agency. The ANH-San Cayetano-1well was drilled in the SJFB southeast of the city of Cartagena (Figure 2) to a total depth of 2314.5 ft (705.5 m). Overall, it consists of interbedded sandstones and mudstones, with sandstone beds decreasing toward the top (Figure 3). In this study, three stratigraphic intervals can be recognized from base to top: Interval 1 (2315-1060 ft): it consists mainly of thin to medium beds of fine to medium-grained sandstones interbedded with structureless or parallel laminated grayish black mudstones with a significant predominance of sandstones over mudstones. The sandstones have scour marks, normal grading, parallel and ripple lamination, and complete and incomplete Bouma sequences. Soft-sediment deformation structures such as convolute and slump folds, and syn-sedimentary faults are common. Locally, medium to thick beds of intraformational breccias composed of angular to sub-angular, poorly sorted mudstone pebbles with sandy matrix are observed. Bioturbation is common, but only with scattered discrete traces (bioturbation index 1; Taylor and Goldring, 1993). Glauconite, plant remains, and pyrite are also identified. Mudstones contain pollen, spores, dinoflagellates, and some calcareous nannofossils, foraminifera (mainly benthic), and indeterminate bivalves. Interval 2 (210-1060 ft): the lithology, structure and texture of the sedimentary rocks are similar to the previous interval, but the proportions of mudstones and sandstones are similar, and there are no intraformational breccias. In addition, occasional occurrences of limestones (mudstones and wackestones) are observed. The mudstones are generally poor in pollen, spores, and dinoflagellates. Calcareous nannofossils and foraminifera (mainly benthic) are more abundant than in the previous interval. Interval 3 (0-210 ft): consists mainly of thin to thick beds of dark gray mudstones, structureless or with parallel lamination, interbedded with some thin beds of medium to fine-grained arkoses and lithic arkoses, with sedimentary structures and bioturbation indexes as in intervals 1 and 2. Mudstones are poor in pollen, spores, and dinoflagellates. Calcareous nannofossils and foraminifera (mainly benthic) vary from rare to abundant.

The ANH-Piedras Blancas-1X well drilled a total depth of 1219 ft (~372 m) of a thick terrigenous succession. It consists of thin to medium beds of mudstones interbedded with sandstones (Figure 3). The sandstones are fine to medium grained and well to moderately sorted. Internally, they show normal and inverse grading, parallel and current ripple laminations, comparable to complete and incomplete Bouma sequences. There are also load structures, ball and pillow, convolute lamination, and syn-sedimentary faults. Locally, charcoal fragments, bivalve remains, gastropods, foraminifera, echinoderms, and brachiopods are observed. Bioturbation is also present. The mudstones are dark gray to black, generally massive or with parallel lamination, often bioturbated (BI between 1 and 4) and calcareous. Some beds contain carbonized fragments, bivalves, gastropods, foraminifera, calcareous nannofossils, ostracods, and marine and terrestrial palynomorphs. Less common are medium to thick beds of intraformational breccias composed of angular to subangular, poorly sorted mudstone and calcareous mudstone pebbles with muddy and sandy matrix.

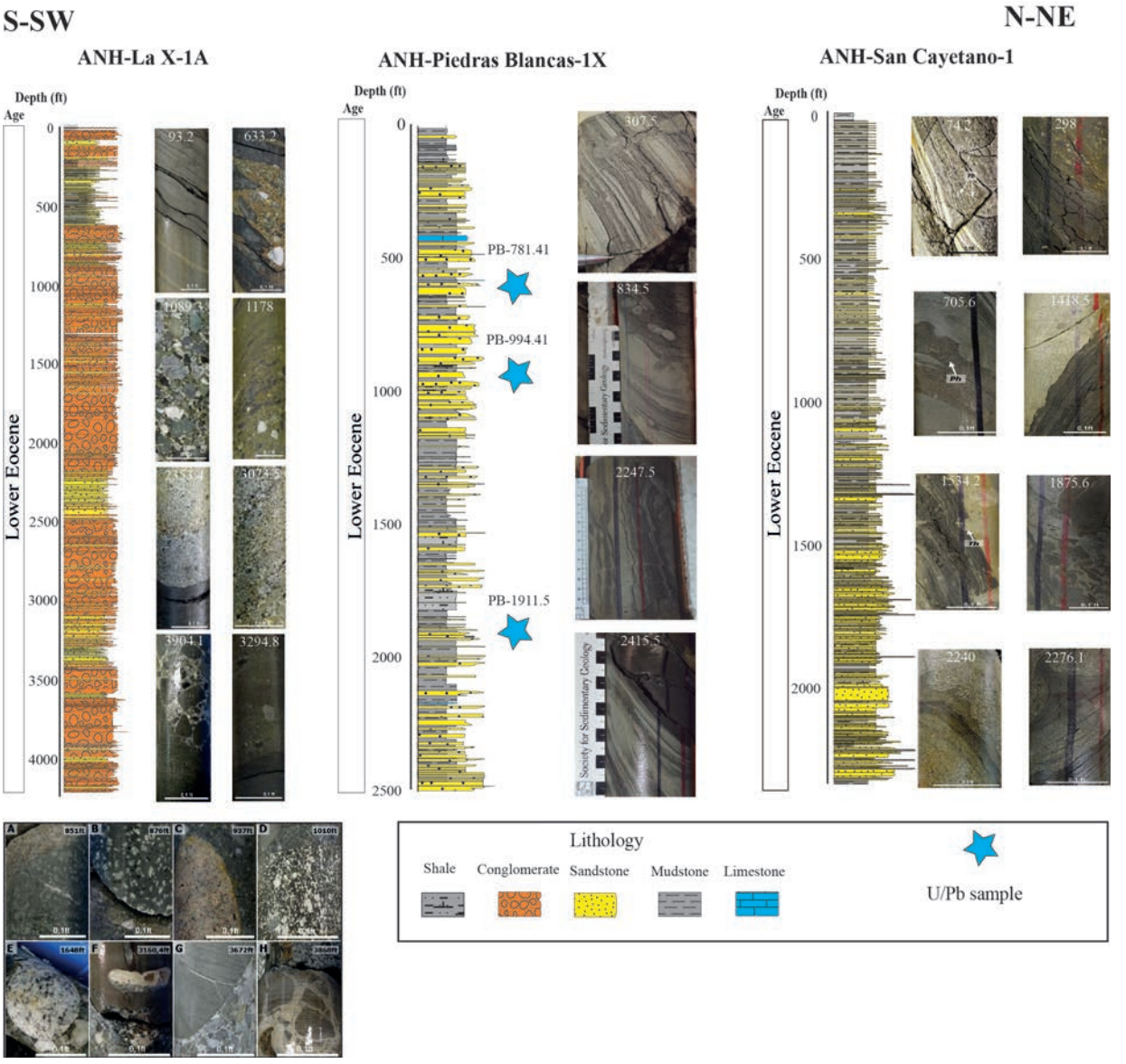

Figure 3. Stratigraphic columns and lithologic features along the studied wells and location of zircon U-Pb geochronology samples. Types of clasts found in the ANH-La X-1A well **A.** and **B.** andesite clasts, **C.** granite clast, **D.** diorite clast, **E.** granite clast, **F.** limestone clast, **G.** sandstone clast, **H.** sedimentary breccia.

The ANH-La X-1A well was drilled in the central part of the SJFB near the city of Montería (Figure 2) to a total depth of ~4133 ft (1260 m). It is generally composed of conglomerates interbedded with sandstones and, to a lesser extent, mudstones (Figure 3). The conglomerates consist of thick to very thick beds of clast or matrix-supported beds; internally they may be structureless, or with crossbedding and imbrication of the clasts. They are mainly polymictic conglomerates of pebbles and cobbles, exceptionally of blocks (> 1m thick), moderately to poorly sorted, with subrounded to rounded clasts, composed of volcanic (andesites, basalts), sedimentary (conglomerates/breccias, shales, limestones, sandstones, cherts), igneous (granites, diorites, and gabbros), and metamorphic

(schists and quartzites) fragments; the matrix is fine to medium sandstone with glauconite. Muddy intraclasts and charred woody debris are common. In some stratigraphic intervals (e.g., 3350-3040 ft and 2440-2140 ft, 810-730 ft), thick beds of medium to very coarse-grained, moderately calibrated sandstones are usual. They may be structureless, or with parallel or cross bedding, and occasionally bioturbated. To a lesser extent, there are thin beds of dark-gray mudstones interbedded with structureless or with parallel lamination, occasionally bioturbated, with sparse palynomorphs (terrestrial and marine), calcareous nannofossils, and benthic foraminifera. A sharp change in facies is noted between 610-0 ft. Towards the base of this interval (610-500 ft), medium to thick beds of fine, medium, and coarse-grained structureless or normal grading, parallel lamination, locally bioturbated, charred organic matter sandstones occur, with commonly muddy intraclasts. Sandstones are interbedded with thin to medium beds of massive or with parallel lamination, bioturbated, gray mudstones. Fossils of terrestrial palynomorphs, calcareous nannofossils, agglutinated benthic foraminifera and indeterminate mollusks are present in minor proportions. Between 500-260 ft in the central part of this interval, there is a predominance of fine to medium beds of massive or parallel laminated, and bioturbated mudstones, interbedded with thin to thick beds of sandstones, with composition and sedimentary structures very similar to those described at the base of this interval. Towards the well top, medium to very thick beds of mainly structureless clast and matrix-supported conglomerates dominate. To a lesser extent, crossbedding, and locally imbricated clasts can be found. The clasts are subrounded to subangular, poorly to moderately sorted, composed of volcanic (andesites), plutonic (granites), and sedimentary (shales, cherts, and sandstones) rock fragments (Figure 3); the matrix is sandy and includes glauconite grains. To a lesser extent, there are thin to medium beds of greenish-gray calcareous mudstones (marls) with parallel lamination and bioturbation, as well as fine to very coarse-grained sandstones with parallel or cross bedding.

Previously proposed ages and depositional environments of the studied wells

For the ANH-San Cayetano-1 well Plata-Torres *et al.* (2023) and Vallejo-Hincapié *et al.* (2023), assigned an early Eocene (Ypresian) age (Figure 4). Based on calcareous nanofossils Vallejo-Hincapié *et al.* (2023) pointed out that the presence of *H. lodoensis, R. dictyoda,* and *S. orphanknolli* indicates that the 277-m-thick interval between 1190 ft (362 m) and 306 ft (97 m) spans Zone NP12 through Subzone NP14a of the Early Eocene Subseries (Ypresian Stage) according to biozonation of Martini (1971). Palynology indicates that the base cannot be older than the Ypresian due to the presence of *Cyclusphaera scabrata, Bombacacidites nacimientoensis, Spirosyncolpites spiralis,* and *Striatopollis catatumbus*. Besides, the presence of nannofossils *Fasciculithus* spp., *Lithoptychius* spp., and *Prinsius* spp., which indicates Paleocene Zones NP7 to NP9 suggest reworking of Paleocene sedimentary rocks.

For the ANH-Piedras Blancas-1X well the co-occurrence of the calcareous nannofossils *H. lodoensis, R. dictyoda,* and *S. orphanknolli* indicates that the sedimentary interval between 1190 ft (362 m) and 279 ft (85 m) in the core spans zones NP12 to NP14a and was deposited between ~53 and ~48.3 Ma (late Ypresian Age) (Vallejo-Hincapié *et al.*, 2019). For the ANH-La X-1A well, Vallejo-Hincapié *et al.* (2023) assigned an early Eocene (Ypresian) age (zones NP11-NP12) to the interval between 995.2 and 138.4 m (3273.84-455.1 ft) based on calcareous nannofossils *T. orthostylus, S. radians, Toweius callosus.* However, they noted that the biostratigraphic age of the upper part of the core (121.9-22.4 m; 622.9-73.6 ft) could not be constrained with nannofossils due to poor recovery of stratigraphic markers. Furthermore, the presence of mudstone clasts embedded in the upper and lower parts of the well with *Fasciculithus clinatus* and *Lithoptychius* spp., which occur in upper Paleocene Zone NP7 and NP9, indicates reworking of Paleocene sedimentary rocks.

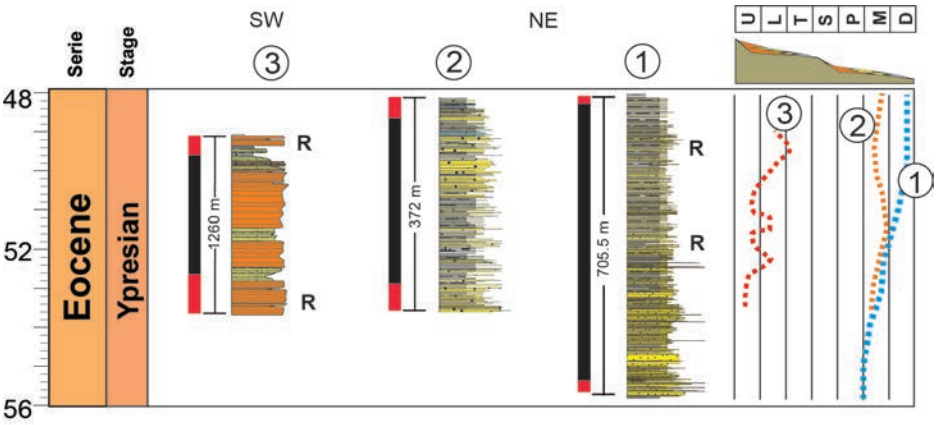

Figure 4. Thickness, chronostratigraphy and paleoenvironments variability along the studied wells based on microfossils and stratigraphic descriptions (ANH-Universidad de Caldas, 2023; Plata-Torres *et al*., 2023; Vallejo-Hincapié *et al*., 2023). 1) ANH-San Cayetano-1 well; 2) ANH-Piedras Blancas-1X well; 3) ANH-La X-1A well. U) Upper fan delta; L) Lower fan delta; T) Shelf/prodelta; S) Slope; P) Proximal submarine fan; M) Middle submarine fan; D) Distal submarine fan. R) Reworked microfossils. Red and black bars indicate absence or presence of biostratigraphic data respectively. SW and NE represent the positions of the wells in the basin.

ANH-Universidad de Caldas (2023) used stratigraphic descriptions, facies analysis, and ichnological data from all three wells to interpret the depositional paleoenvironments (Appendix A–D). These data indicate that, in the ANH–La X-1A well (Appendix B), the deposits correspond to an upper fan-delta environment grading upward into lower fan-delta and prodelta/shelf deposits. In the ANH–Piedras Blancas-1X and ANH–San Cayetano-1 wells (Appendix C and D), a middle submarine fan environment was interpreted, transitioning upward into distal fan deposits, particularly in the San Cayetano well. A comparison of the three wells reveals contrasting paleoenvironments from south to north, with shallower marine deposits toward the south and deeper marine environments toward the north (Figure 4).

Sampling and Methods

To gain new insights into the paleogeography and magmatism of the SJFB during the Eocene, we used a multi-proxy approach including petrography and zircon U/Pb geochronology on samples from the ANH-Piedras Blancas-1X, ANH-La X-1A, and ANH-San Cayetano-1 wells. Three-hundred twenty-eight very fine to conglomeratic sandstones were selected from the three wells. 200-300 g were taken from the well cores for making thin sections, and 500-800 g per sample from three sandstones from the ANH-Piedras Blancas-1 for U/Pb geochronology (Figure 3).

Petrography

Petrographic analyses of sandstones were performed using the Gazzi-Dickinson method (Ingersoll *et al*., 1984). Three hundred (300) points per thin section, including framework, interstitial material, and pores, were counted to evaluate the modal composition and textural parameters such as grain sorting and roundness. Counted points were normalized to percentages and presented in the Appendix E section. Particles less than 0.065 mm in diameter were classified as matrix, while larger particles were considered as lithics or grains. Sandstones were stained for feldspar recognition. The classification scheme of Folk (1980) was implemented. Tectonic provenance classification was performed on sandstones with matrix, cement and organic matter content <30% (Dickinson, 1985). Petrographic analyses were carried out at the Instituto de Investigaciones en Estratigrafía (IIES), Universidad de Caldas and the Universidad Industrial de Santander (UIS).

Zircon U/Pb geochronology

As part of the mineral separation process, zircon concentrates were obtained for U-Pb geochronology. Detrital zircons were mounted in doble stick tape and covered with epoxy resin to make plugs, subsequently polished, and U-Pb dated by laser ablation inductively coupled plasma mass spectrometry (LA-ICP-MS) method (Košler and Sylvester, 2003; Gehrels, 2011), using a Nu-Plasma ICP-MS equipped with three ion counters and 12 Faraday detectors. Analyses were performed at the department of geological sciences at the University of Florida. Overall, samples presented low zircon yields (~40-100), therefore, the total number of zircons was mounted and dated. Complete description of methods used for U/Pb analysis can be found in Barbosa-Espitia *et al*. (2019).

Results

Petrography

Sixty-three sandstone samples were analyzed from the ANH-San Cayetano-1 well (Appendix E). Based on stratigraphic position, Quartz (Q), Feldspar (F) and Lithics (L) content according to Folk (1980), and compositional maturity index (CMI) (Suttner and Dutta, 1986) (Figure 5A), this well can be divided into three domains. The first domain (between 44.5-714.3 ft) is composed mainly of fine-medium grained, well-moderately sorted arkoses and few very fine-fine grained, well sorted lithic arkoses (Figure 5B) with CMI varying from 0.5 to 2.4 (Figure 5A). The most abundant constituent is subangular-subrounded quartz with monocrystalline quartz being the dominant constituent (43.7-13.3%) compared with polycrystalline quartz (0-5.7%); followed by subangular feldspars, dominated by K-spar (18.8-6%) and less abundant well-preserved plagioclase (16.3-7%). Lithic fraction is the least abundant component. It is composed of subrounded volcanic rocks (basalts and andesites) from 0 to 6.8%, rounded sedimentary rocks (sandstones and mudstones) from 0 to 2.6%, and subrounded metamorphic rocks (quartzites and schists) from 0 to 2.7% (Figure 5C). Chlorite (1.6-6.3%), muscovite mica (0-1.3%), chert (1.3-7.3%), microfossils (0-2.7%), authigenic glauconite (0-3.5%), organic matter (0-1.9%), heavy (tourmaline and zircon) (0-1.3%) and opaque minerals (0-10.8%) are also present. Clay and calcareous matrix vary from 0-36.6%, iron cement is not common but can reach up to 6.4% in the middle part of the domain, porosity varies from 0-25%. Sericitization in plagioclase and slight kaolin alteration in K-felspar along with monocrystalline quartz overgrowths are common. On the QmFL diagram samples from this domain plot mainly in the basement uplift field with a few samples in the transitional continental and dissected arc fields (Figure 5D). The second domain between 714.3-1114.2 ft is composed of fine grained, well sorted arkoses and fine-medium grained, moderately-well sorted lithic arkoses (Figure 5B) with CMI varying from 0.5 to 2.4 (Figure 5A). The most abundant constituent is subrounded-subangular feldspar with plagioclase ranging from 23.3 to 4.7% and less abundant K-spar (15.7-5.9%); followed by subrounded-subangular quartz dominated by monocrystalline quartz (15.4-30%) compared with polycrystalline (0.5-5.1%). Lithic content is the least abundant component, which is composed of subrounded volcanic rocks (basalts and andesites) from 0 to 7.7%, subrounded sedimentary rocks (sandstones and mudstones) from 0 to 5.1%, and subrounded to subangular metamorphic rocks (quartzites + schists) from 0 to 2.8% (Figure 5C). Additional constituents are chlorite (0-6.8%), muscovite mica and sporadic biotite (0-0.5%), chert (0.5-3.2%), microfossils (0-8.8%), authigenic glauconite (0-1.6%), organic matter (0-1.5%), heavy minerals (zircon, and sporadic tourmaline and epidote) (0-2.3%), and opaques (0-7%). Clay and calcareous matrix varies from 0 to 38.9%, and porosity varies from 0-25%. Sericitization in plagioclase crystals, chloritized volcanic lithics, as well as sericitized and epidotized plutonic lithics are common. Cement is mainly non-ferruginous and ferruginous carbonate, and occasionally siliceous. In the QmFL diagram samples from this domain plot mainly in the basement uplift and transitional continental fields with a few samples in the mixed and dissected arc fields (Figure 5). The third domain between 1114.2-2298.4 ft, is composed mainly of fine-medium grained, moderately sorted feldspathic litharenites and fine-medium grained, moderately-poorly sorted lithic arkoses with few fine-medium grained, well-poorly sorted arkoses and litharenites with CMI varying from 0.7 to 1.7. The most abundant constituent is subrounded-subangular quartz, being monocrystalline quartz the dominant constituent (37.7-14%) compared with polycrystalline quartz (2-14.7%); followed by subangular-subrounded feldspars, dominated by plagioclase (16.8-3.3%) and less abundant K-spar (15.3-0.7%). Lithic fraction is the least abundant component. It consists of subangular-subrounded plutonic rocks (felsic plutonics) from 0 to 15.7%, subangular-subrounded volcanic rocks (basalts and andesites) from 0 to 14.7%, subangular-subrounded sedimentary rocks (sandstones and mudstones) from 0 to 3.7%, and subangular-subrounded metamorphic rocks (quartzites and schists) from 0 to 5% (Figure 5D). Authigenic kaolinite/chlorite (0-3%), muscovite mica and occasionally biotite (0-12.7%), chert (0-19.3%), microfossils (0-0.7%), authigenic glauconite (0-31.7%), heavy minerals (zircon, tourmaline, epidote and pyroxene) (0-3%), and opaques (0-2.7%) are also present. Clay and calcareous matrix varies from 0 to 28%, iron cement is most common compared with the other domains reaching up to 62.3% in the middle part of the domain; porosity varies from 0-28.7%. Sericitization in plagioclase crystals, chloritized volcanic lithics, as well as sericitized and epidotized plutonic lithics are common. Cement is mainly non-ferruginous and ferruginous carbonate, and occasionally siliceous. In the QmFL diagram samples from this domain plot mainly in the mixed and dissected arc fields with a few samples in the basement uplift, transitional arc and transitional recycled (Figure 5D).

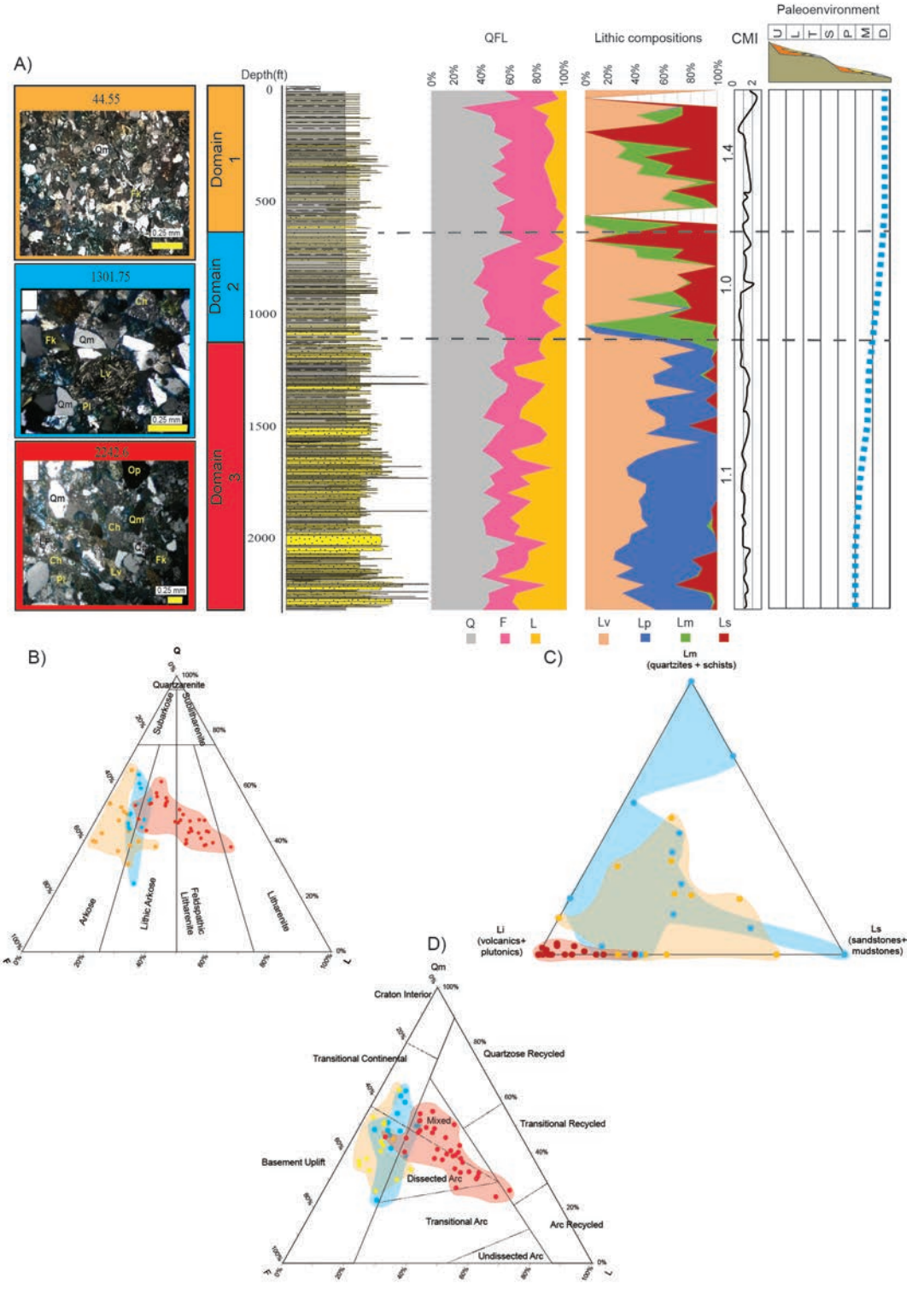

Figure 5. A. QFL, lithics compositional, compositional maturity index (CMI), and paleoenvironmental variability along the ANH-San Cayetano-1 well; and petrographic characteristics of the compositional domains. Numbers in de CMI column represent average CMI of each domain. **B.** Modal classification. **C.** Lithic characteristics and domains grouping. **D.** Provenance discrimination diagrams from the studied wells. Q-F-L: quartz-feldspar-lithics; Qm: monocrystalline quartz; Qt: total quartz; L: lithics; Lv: volcanic lithics; Lp: plutonic lithics; Lm: metamorphic lithics; Ls: sedimentary lithics; Li: igneous lithics; U: Upper fan delta; L: Lower fan delta; T: Shelf/prodelta; S: Slope; P: Proximal submarine fan; M: Middle submarine fan; D: Distal submarine fan.

Ninety-six sandstone samples were analyzed from the ANH-Piedras Blancas-1X well (Appendix E). Based on its stratigraphic position, Quartz (Q), Feldspar (F) and Lithics (L) content, and the CMI (Figure 6A), this well can be divided into three domains. The first domain (between 250.6-1196.6 ft) is composed mainly of very fine-medium grained, well-moderately sorted feldspathic litharenites and lithic arkoses (Figure 6B) with CMI varying from 0.5 to 2.4 (Figure 6A). The main constituent is the lithic fraction, which is composed of subangular plutonic rocks (felsic plutonics) from 0-10.7%, subangular-subrounded volcanic rocks (basalts and andesites) from 0-10.7%, subrounded sedimentary rocks (sandstones, mudstones and limestones) from 0 to 3-8.7%, and subangular metamorphic rocks (quartzites and schists) from 0 to 2.6% (Figure 6C), followed by angular-subrounded quartz, which is dominated by monocrystalline quartz from 31 to 8% and polycrystalline quartz from 0.3 to 15.7%. The feldspar is dominated by well-preserved plagioclase ranging from 4 to 16.7% and K-spar ranging from 0 to 5.3%. Additional components are muscovite mica (0.3-12%), chert (0.3-12%), microfossils (0-14.3%), subrounded glauconite grains (0-2%), and organic matter (0.3-6%). Clay and calcareous matrix varies between 0-18.7%, siliceous cement ranks between (0-3%), and porosity varies from 0-1%. In the QmFL diagram samples from this domain plot mainly in the transitional arc and dissected arc fields with a few samples in the mixed and transitional fields (Figure 6D). The second domain between 1196.6-1715.5 ft, is composed of very fine-medium grained, well-moderately sorted felspathic litharenites, litharenites and a few subarkoses and sublitharenites (Figure 6B) with CMI varying from 2.1 to 6.4 (Figure 6A). The most abundant constituent is subangular-subrounded quartz, with monocrystalline quartz being the dominant constituent (14.3-39.3%) compared with polycrystalline quartz (0.3-3.7%); followed by the lithic fraction, dominated by subrounded volcanic rocks (basalts and andesites) from 0 to 9.7%, subrounded-subangular plutonic rocks (felsic plutonics) from 0 to 11.3%, subrounded sedimentary rocks (sandstones, mudstones, limestones) from 0 to 6.9%, and subangular metamorphic rocks (quartzites and schists) from 0 to 4% (Figure 6C). Subangular-subrounded feldspar is the least abundant fraction with plagioclase from 2.3 to 12% and less abundant K-spar (0-2.3%). Muscovite micas (0.3-13%), chert (0-12.7%), microfossils (0.7-9.7%), subrounded glauconite grains (0-1.3%), and organic matter (0.3-4.7%) are also present. Clay matrix varies between 0-36.7%, siliceous and calcareous cement varies between 0.3 and 5.7%, and porosity varies from 0-3%. In the QmFL diagram samples from this domain plot mainly in the transitional recycled and quartzose recycled field and a sample in the craton interior field (Figure 6D). The third domain between 1715.5-2476.5 ft, is composed mainly of fine-very fine grained, moderately sorted feldspathic litharenites and lithic arkoses with a few arkoses and litharenites (Figure 6B) with CMI varying from 0.7 to 4.2 (Figure 6A). The most abundant constituent is subangular-subrounded quartz, being monocrystalline quartz the dominant constituent (17-32.3%) compared with polycrystalline quartz (0-5%); followed by the lithic fraction, which is composed of subangular-subrounded sedimentary rocks (sandstones and mudstones) from 0 to 6.3%, subangular-subrounded volcanic rocks (basalt and andesites) from 0 to 10.3%, plutonic rocks (felsic) from 0 to 5.3%, and subangular-subrounded metamorphic rocks (quartzites and schists) from 0 to 4.3% (Figure 6C). Subangular-subrounded feldspar is the least fraction with plagioclase from 2.7 to 16.3% and less abundant K-spar (0-2%). Additional components are micas (1-12.7%), chert (0-14.7%), microfossils (2-13%), glauconite (0-1.7%), and organic matter (1-10.7%). Clay matrix varies from 5.7 to 48.7%, siliceous and calcareous cement varies from 0 to 4.3%, and porosity varies from 0 to 3%. Occasionally, ferric calcite replaces both quartz and plagioclase grains. Authigenic mineral such as pyrite, chlorite and iron oxides also are present along the well. In the QmFL diagram, samples from this domain plot mainly in the transitional arc, dissected arc, and mixed fields, with two samples in the quartzose recycled field (Figure 6D).

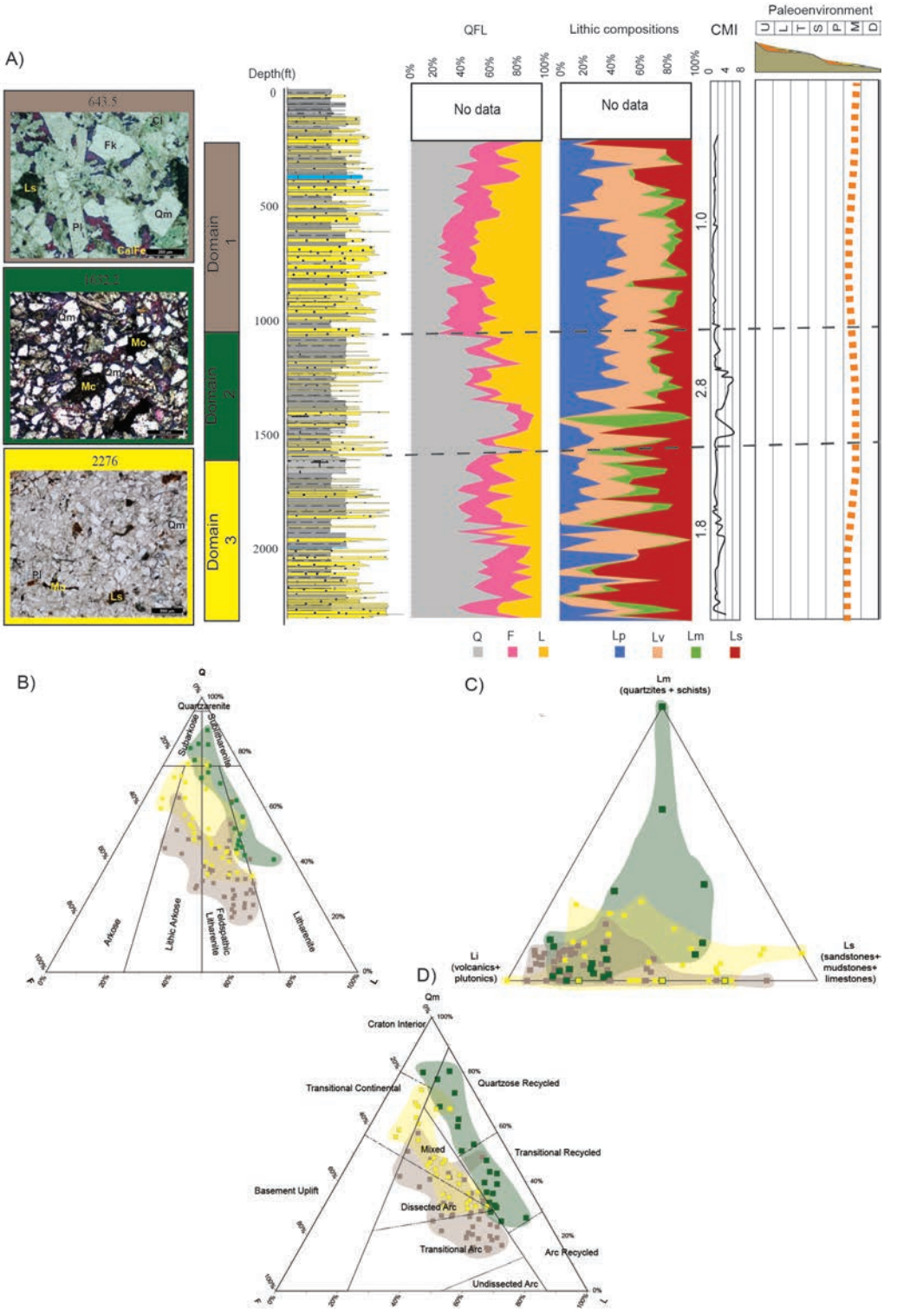

Figure 6. A. QFL, lithics compositional, compositional maturity index (CMI), and paleoenvironmental variability along the ANH-Piedras Blancas-1X well; and petrographic characteristics of the compositional domains. Numbers in de CMI column represent average CMI of each domain. **B.** Modal classification. **C.** Lithic characteristics and domains grouping. **D.** Provenance discrimination diagrams from the studied wells. Q-F-L: quartz-feldspar-lithics; Qm: monocrystalline quartz; Qt: total quartz; L: lithics; Lv: volcanic lithics; Lp: plutonic lithics; Lm: metamorphic lithics; Ls: sedimentary lithics; Li: igneous lithics; U: Upper fan delta; L: Lower fan delta; T: Shelf/prodelta; S: Slope; P: Proximal submarine fan; M: Middle submarine fan; D: Distal submarine fan.

One hundred and fifty-one sandstone samples were analyzed from the ANH-La X-1A well (Appendix E). Although there is not a clear compositional difference along the entire well, based on its stratigraphic position, a little increment in the feldspar content towards top of the borehole, and the CMI (Figure 7A), this well can be divided into two domains. The first domain (between 0-1563 ft) is composed mainly of very poorly-poorly sorted, conglomeratic to well-moderately sorted, fine grained litharenites, feldspathic litharenites and minor lithic arkoses (Figure 7B) with CMI varying from 0.4 to 1.0 (Figure 7A). The main component is the lithic fraction, which consists of subrounded-subangular volcanic rocks (basalts, andesites and minor tuffs) from 2.3 to 32.4%, subrounded-subangular plutonic rocks (felsic plutonics) from 3 to 18.7%, subrounded sedimentary rocks (sandstones and mudstones) from 0.7 to 11.7%, and subrounded-subangular metamorphic rocks (quartzites and schists) from 2.4 to 16.7%, followed by angular-subangular quartz, which is dominated by monocrystalline quartz from 4 to 29.7% and polycrystalline quartz from 0.3 to 18%. Feldspar is dominated by fresh angular-subangular K-spar from 1.3 to 12.7% and well-preserved plagioclase from 0 to 10.7%. Additional constituents are biotite and muscovite micas (0-16%), chert (0-6.3%), microfossils (0-8.7%), glauconite (0-0.7%), organic matter (0-7.3%). Clay and calcareous matrix varies between 0-26%, iron cement from 0 to 29%, and porosity from 0 to 27.3%. Volcanic lithics are frequently devitrified and occasionally replaced by calcite. Sericitization in plagioclase and epidotization in plutonic lithics are common. Cement occurs as patches of no ferric carbonates. In the QmFL diagram samples from this domain plot mainly in arc recycled, and transitional recycled fields with few samples in dissected arc, transitional arc and mixed fields (Figure 7D). The second domain (1563-4133.1 ft) is composed of well-moderately sorted, fine to very poorly-poorly conglomeratic litharenites and feldspathic litharenites (Figure 7B) with CMI varying from 0.4 to 2.5 (Figure 7A). The main constituent is the lithic fraction, which is composed of volcanic rocks (basalts and andesites) from 1 to 41.3%, plutonic rocks (felsic) from 0.7 to 18.3%, metamorphic rocks (quartzites and schists) from 0.3 to 23.7%, and sedimentary rocks (sandstones-mudstones) from 0-19.7%; followed by quartz, being monocrystalline quartz the dominant constituent (2.4-31.8%) compared with polycrystalline quartz (0-35.3%). Feldspar is dominated by K-spar from 0.5 to 10.3% and plagioclase from 0 to 8.3%. Micas (0-0.7%), chert (0-11.3%), microfossils (0-0.7%), organic matter (0-1.7%), heavy minerals (0-3.3%), and opaques (0-4%) are also present. Clay and calcareous matrix varies from 0 to 41%, iron cement from 0 to 3.3%, and porosity from 0 to 19.3%. In this domain, three types of cement were identified: calcareous, pyritic and chloritic. Volcanic lithics are frequently devitrified and occasionally dissolved or chloritized, whereas dissolution and/or sericitization occur in plagioclase. Dissolution is occasionally present in quartz as well. Cement occurs as patches of carbonates and/or mineral replacement by chlorite. In the QmFL diagram samples from this domain plot mainly in the arc recycled, and transitional recycled fields with a few samples in transitional and dissected arc fields (Figure 7D).

Zircon U/Pb geochronology

Three sandstone samples were analyzed from the Eocene strata of the SJFB. Specifically, we dated three samples from the Lower Eocene ANH-Piedras Blancas-1X well (Figure 8 and Appendix F). Two samples correspond to sandstones (PB-994.91 and PB-1911.5), and the other corresponds to a clast of sandstone-mudstone from a conglomerate (PB-781.41). We dated the sandstones and conglomerate to check for consistency in the provenance signal of fine and coarse grain fractions. There is no significant variation in the zircon ages analyzed from samples PB-994.91 (n:44) and PB-1911.5 (n:99). The population with the highest probability is the Late Cretaceous (ca. 70-90 Ma), followed by the Permian-Triassic (230-290 Ma) and minor Precambrian populations (Figure 8). A few Eocene zircons (3) were also found within these two samples, yielding a maximum depositional age of 53.2±1.2 Ma (Ypresian) for the studied sequence (Figure 8). Sample PB-781.41 (n:42) shows a single Late Cretaceous-Paleocene population (60-75 Ma) (Figure 8).

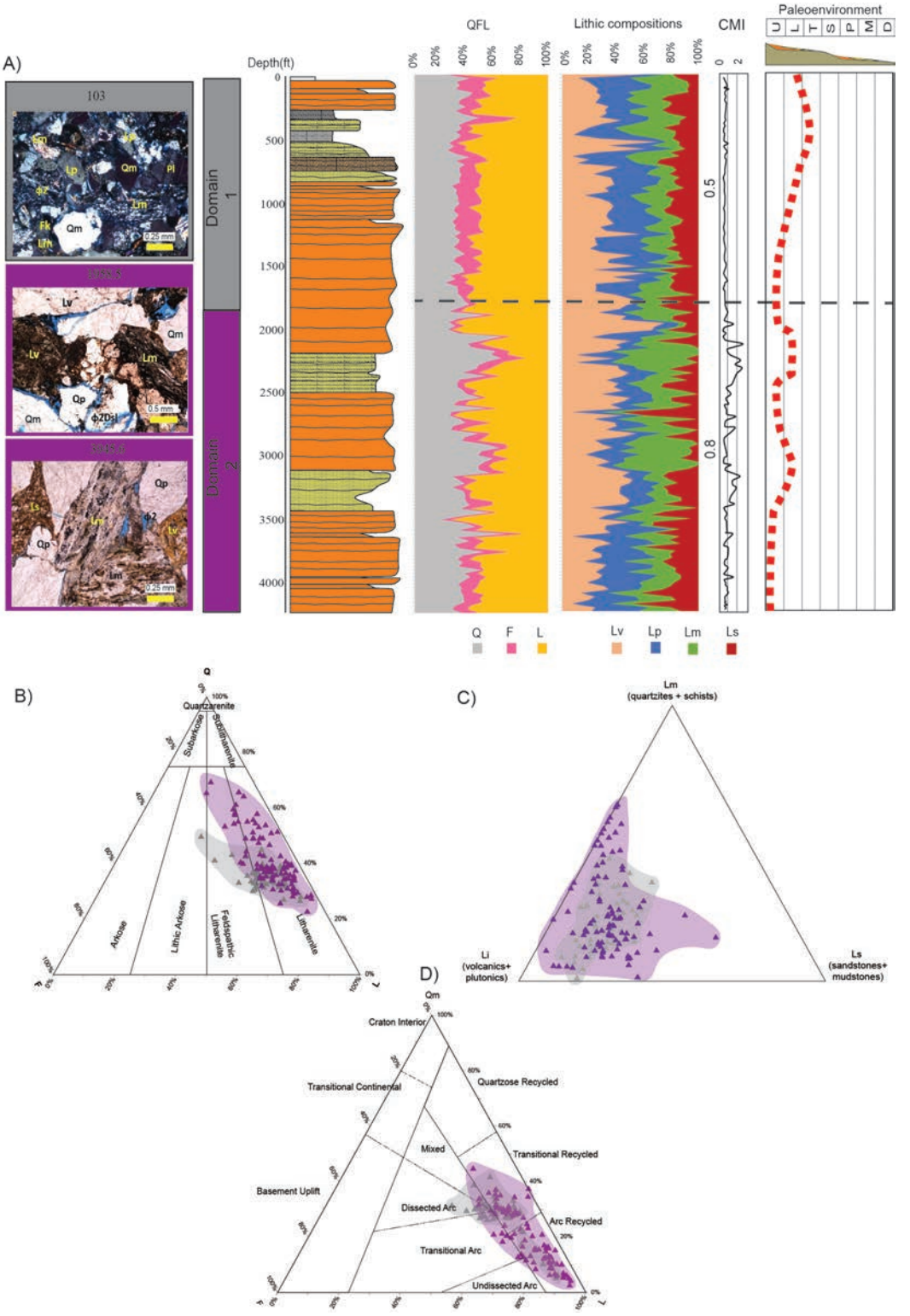

Figure 7. A. QFL, lithics compositional, compositional maturity index (CMI), and paleoenvironmental variability along the ANH-La X-1A well; and petrographic characteristics of the compositional domains. Numbers in de CMI column represent average CMI of each domain. **B.** Modal classification. **C.** Lithic characteristics and domains grouping. **D.** Provenance discrimination diagrams from the studied wells. Q-F-L: quartz-feldspar-lithics; Qm: monocrystalline quartz; Qt: total quartz; L: lithics; Lv: volcanic lithics; Lp: plutonic lithics; Lm: metamorphic lithics; Ls: sedimentary lithics; Li: igneous lithics; U: Upper fan delta; L: Lower fan delta; T: Shelf/prodelta; S: Slope; P: Proximal submarine fan; M: Middle submarine fan; D: Distal submarine fan.

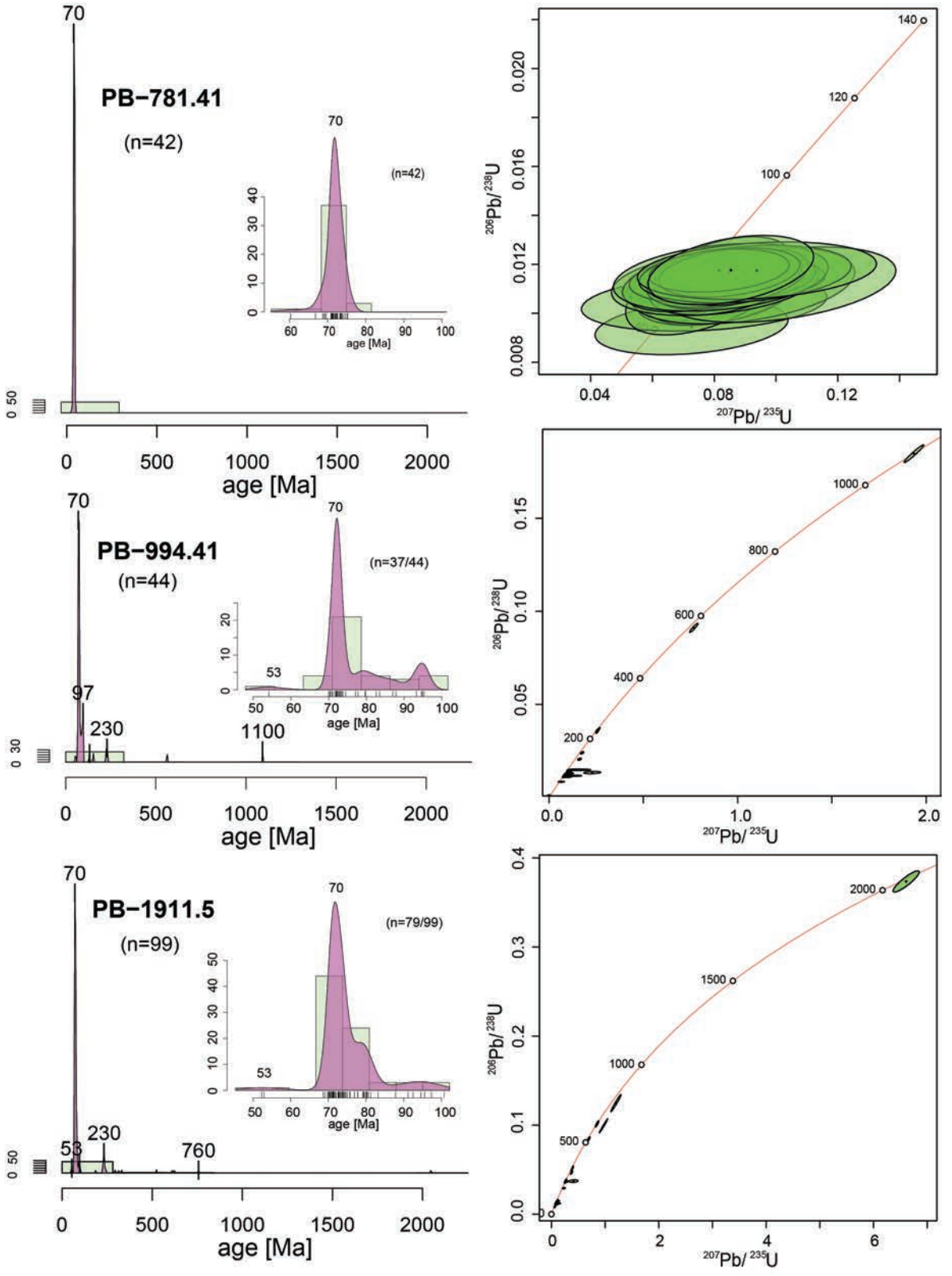

Figure 8. Kernel density plot and Concordia diagrams for the geochronological results of the studied samples, all of them collected in the ANH-Piedras Blancas-1X well. The inner part of the Kernel density plots shows the age distribution between 100-0 Ma.

Discussion

Age of the studied wells

A maximum depositional age of 53.2±1.2 Ma U/Pb obtained in this study for the Piedras Blancas-1 well agrees with a not older than Lower Eocene age for this sequence. Though, only the Piedra Blancas-1 well was dated, biostratigraphic studies in the three studied wells (Plata-Torres *et al*., 2023; Vallejo-Hincapié *et al*., 2023) indicate that these rocks were deposited during the Lower Eocene (Ypresian) (Figure 4). Therefore, they can be correlated chronostratigraphically despite lithologic differences and distance among them (~150 km between La X-1A well and San Cayetano-1 and Piedras Blancas-1 wells).

Vertical compositional variability of the studied wells during Lower Eocene

The sandstone petrographic results for the three studied wells show similarities but also some differences among them. For the ANH-San Cayetano-1 well, three sandy domains were recognized, changing from feldsphatic litharenites towards the well bottom to arkoses toward the well top (Figure 5). The shift is also represented by a decrease in lithics towards the top (Figure 5). Lithics in the feldsphatic litharenite domain are characterized by a dominance of volcanic and plutonic fragments, which represent 80-100% of the lithic fraction (Figure 5). By contrast, metamorphic and sedimentary lithic fractions increase in the other two domains, highlighting the change in provenance and/or depositional conditions between the lower and upper portion of this well. This change in composition from an igneous lithic domain to a more sedimentary-metamorphic felspathic domain is also reflected in the provenance, which changes from an arc related to a basement uplift related tectonic provenance (Figure 5). This compositional maturity shift also appears to correlate with a progressive base to top switch in the paleoenvironment from a shallow to a deeper marine environment (Figure 5), suggesting that the compositional shift may be controlled by the distance from the sedimentary source to the depositional area, with the deeper domain (first domain) being more compositional mature according to the CMI (average CMI: 1.4) compared to the shallower ones (second and third domains, average CMI: 1.1-1.0 respectively) (Figure 5A and Appendix E).

Three sandstones domains were recognized for the ANH-Piedras Blancas-1X well (Figure 6). These domains show a mixture of compositions including feldspatic litharenite-lithic arkoses towards the base and top of the well, and litharenites-subarkoses in the middle part (domain 2). Metamorphic and sedimentary lithics are more prominent towards the base of the well, while plutonic and volcanic fragments increase towards the top. Mixed compositions are also evident in the provenance, including dissected arc, mixed, and transitional continental sources towards the bottom of the well, transitional recycled-quartzose recycled sources towards the middle of the well, and transitional arc-mixed sources towards the top of the well. These diverse compositions indicate an interaction of varied sediment sources of sediments during the Ypresian. Small changes in the paleoenvironment along the well also appear to control the compositional maturity of the sandstones being the deeper domain 2, the most compositional mature (average CMI: 2.8) (Figure 6A and Appendix E).

For the ANH-La X-1A well, there is not much compositional variability between the two identified domains, maintaining a mixture of litharenites and feldspathic litharenites and a provenance dominated by arc recycled and transitional recycled sources (Figure 7). Compositional consistency is also evidenced by the lithic fraction, which does not show significant changes in the amount of volcanic, plutonic, sedimentary and metamorphic fragments found along the well (Figure 7A). This compositional consistency indicates that there were no major changes in provenance sources or sediment yielding throughout the Ypresian. Paleoenvironments in this well vary from lower (base) to upper (top) fan delta, representing shallower marine conditions compared to the other two wells. CMI for the domain 1 (deeper paleoenvironment) is 0.53, meanwhile for domain 2 (shallower paleoenvironment) is 0.85 (Figure 7A). This is contrasting compared with the other two wells, where the CMI tend to increase with deeper environments. The compositional maturity behavior observed in this well may suggest that, in shallower paleoenvironments such as fan deltas, compositional

maturity is less influenced by the depositional setting.

Overall, the most prominent features of each well are the presence of arkoses towards the top of the ANH-San Cayetano-1 well, the presence of a quartzose fraction composed of subarkoses and sublitharenites in the middle (domain 2) of the ANH-Piedras Blancas-1X well, and the prominent dominance of litharenites along the entire ANH-La X-1a well. Another observation is that the average CMI for each well seems to be controlled by the paleoenvironment, since the sandstones from ANH-Piedras Blancas-1X and ANH-San Cayetano-1 (deeper marine environments) are more compositional mature (CMI: 1.7 and 1.2, respectively) compared to those from the shallower ANH-La X-1a well (CMI: 0.78) (Appendix E).

Provenance of the Lower Eocene strata of the SJFB

Petrographic results presented in this study show diverse sources of detrital components According to the ternary classification diagrams of Dickinson (1985) these rocks sources can be associated with different stages of magmatic arcs, cratonic areas and orogenic massifs (Figures 5, 6 and 7). Based on the lithic compositions found, the potential sources of sediments include sedimentary (sandstones, mudstones and limestones), igneous (intermediate-felsic plutonic and basaltic-intermediate volcanic rocks) and low grade metamorphic (schist and quatzites) provinces (Figures 5, 6 and 7). The poor sorting, the angular to sub-angular shape of the detritus and the preservation of unstable components (volcanic clasts, fresh feldspars and micas) suggest that these provinces were proximal, the material was rapidly buried and experienced a limited residence time within an active sedimentary system. Proximal low grade metamorphic and plutonic-volcanic igneous rocks are present in the basement of the LMV (Figure 9). Furthermore, U-Pb ages of the main detrital peaks (Cretaceous-Eocene and Permian-Triassic) reported for the Lower Eocene in this and previous studies (Abreu, 2009; Cardona *et al*., 2012; Mora *et al*., 2017; Osorio-Granada *et al*., 2020) are similar to the Permian Triassic metamorphic and igneous Cretaceous-Triassic LMV basement (Montes *et al*., 2010; Silva-Arias *et al*., 2016; Mora-Bohórquez *et al*., 2017) (Figure 9). These two pieces of evidence suggest that the metamorphic and igneous provinces in the basement of the LMV may be the main rock source of the sandstones and conglomerates associated with the Lower Eocene infill of the SJFB (Figure 9). More distant rock sources with ages and compositions similar to LMV basement and surrounding areas include the CC and SNSM (e.g., Vinasco *et al*., 2006; Cardona *et al*., 2010a, 2010b; Ibañez-Mejía *et al*., 2010; Montes *et al*., 2010; Villagómez *et al*., 2011a; Cochrane *et al*., 2014; Piraquive *et al*., 2022) (Figure 9 and 10). Thermochronological studies suggest that these massifs underwent high exhumation rates during the Eocene (Restrepo-Moreno *et al*., 2009; Cardona *et al*., 2011b; Villagómez *et al*., 2011b; Parra *et al*., 2020); therefore, the presence of some sediments in the SJFB coming from these massifs cannot be completely excluded. The presence of cherts, sandstones and mudstones with minor limestones suggests denudation of a sedimentary cover. The most proximal source of sedimentary rocks similar to those sedimentary lithics found in the studied wells correspond to Cretaceous-Paleocene rocks at the SJFB (Figure 9). A reworked mudstone clast with Paleocene nannofossils in the ANH-LA X-1A and ANH-San Cayetano 1X wells (ANH-Universidad de Caldas, 2023; Vallejo-Hincapié *et al*., 2023), along with Cretaceous-Paleocene U-Pb ages within the clast dated in this study from the Piedras Blancas-1X well (sample PB-781.41), suggest that sedimentary sources can be associated mainly with Cretaceous-Paleocene sedimentary units deposited within the SJFB (e.g., Cansona and lower part of the San Cayetano formation) that were subsequently eroded and redeposited during the Eocene. The lack of paleocurrents information from the studied wells does not allow to know the exact location of this source because Cretaceous-Paleocene sedimentary rocks have been found westward and eastward of the basin, so that none of these possibilities can be ruled out. Additional minor sources of sediments can be found in the U-Pb detrital record reported in this and previous studies (Figure 10), corresponding to Jurassic and Proterozoic minor peaks. These sources may be related to distant sources like the San Lucas massif and the SNSM, where igneous Jurassic and Proterozoic high-grade metamorphic rocks were reported (e.g., Piraquive *et al*., 2022; Gómez *et al*., 2023) (Figure 10) or to reworked Cretaceous-Paleocene sedimentary rocks nearby.

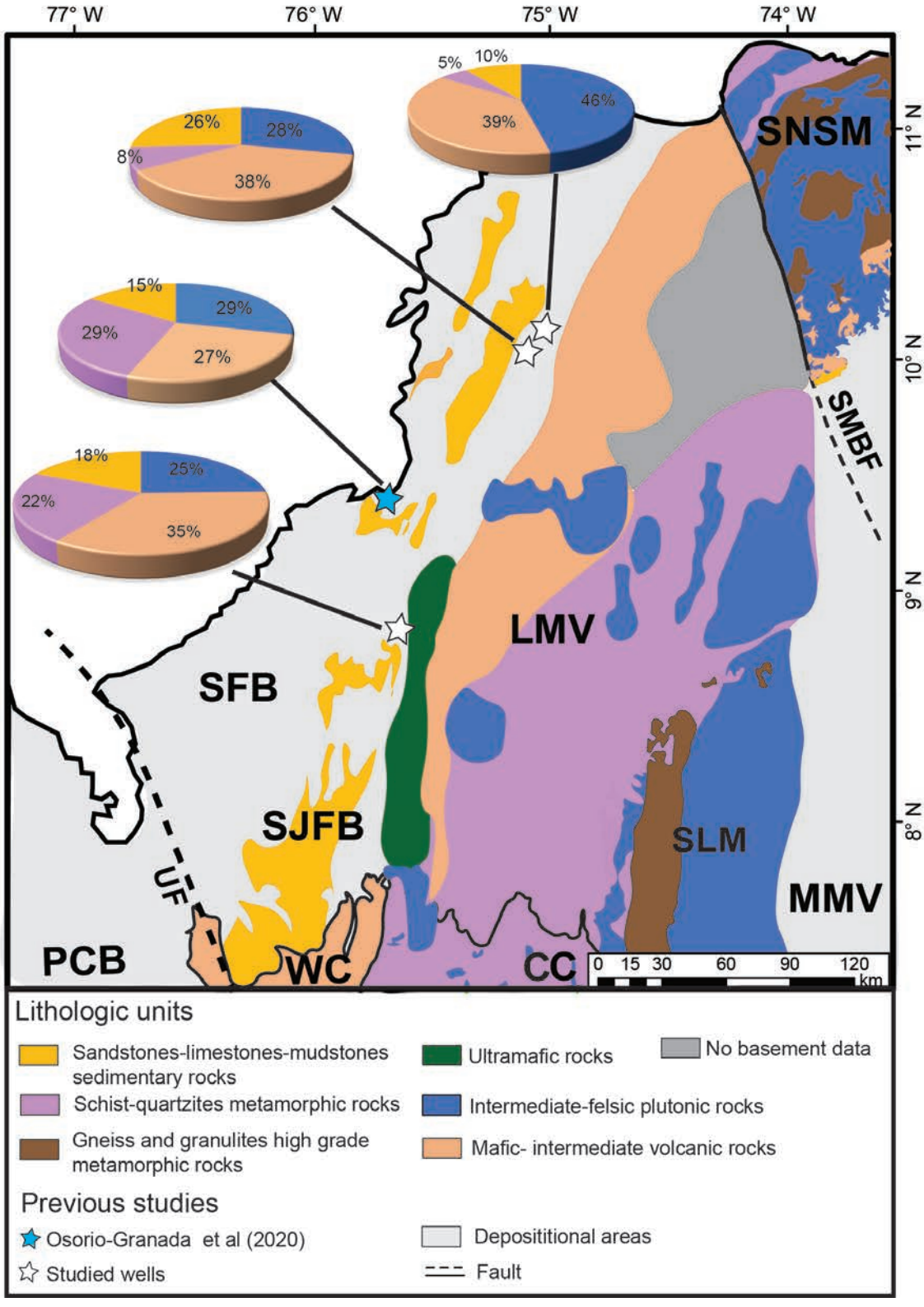

Figure 9. Lithologic map showing the main sedimentary sources from the regions nearby the SJFB and average lithic compositions for each studied well and ANH-San Antero-1X (Osorio-Granada *et al.*, 2020). UF: Uramita fault; SLM: San Lucas Massif; SMBF: Santa Marta-Bucaramanga fault; SFB: Sinú fold belt; LMV: Lower Magdalena Valley; MMV: Middle Magdalena Valley; SNSM: Sierra Nevada de Santa Marta; WC: Western Cordillera; CC: Central Cordillera.

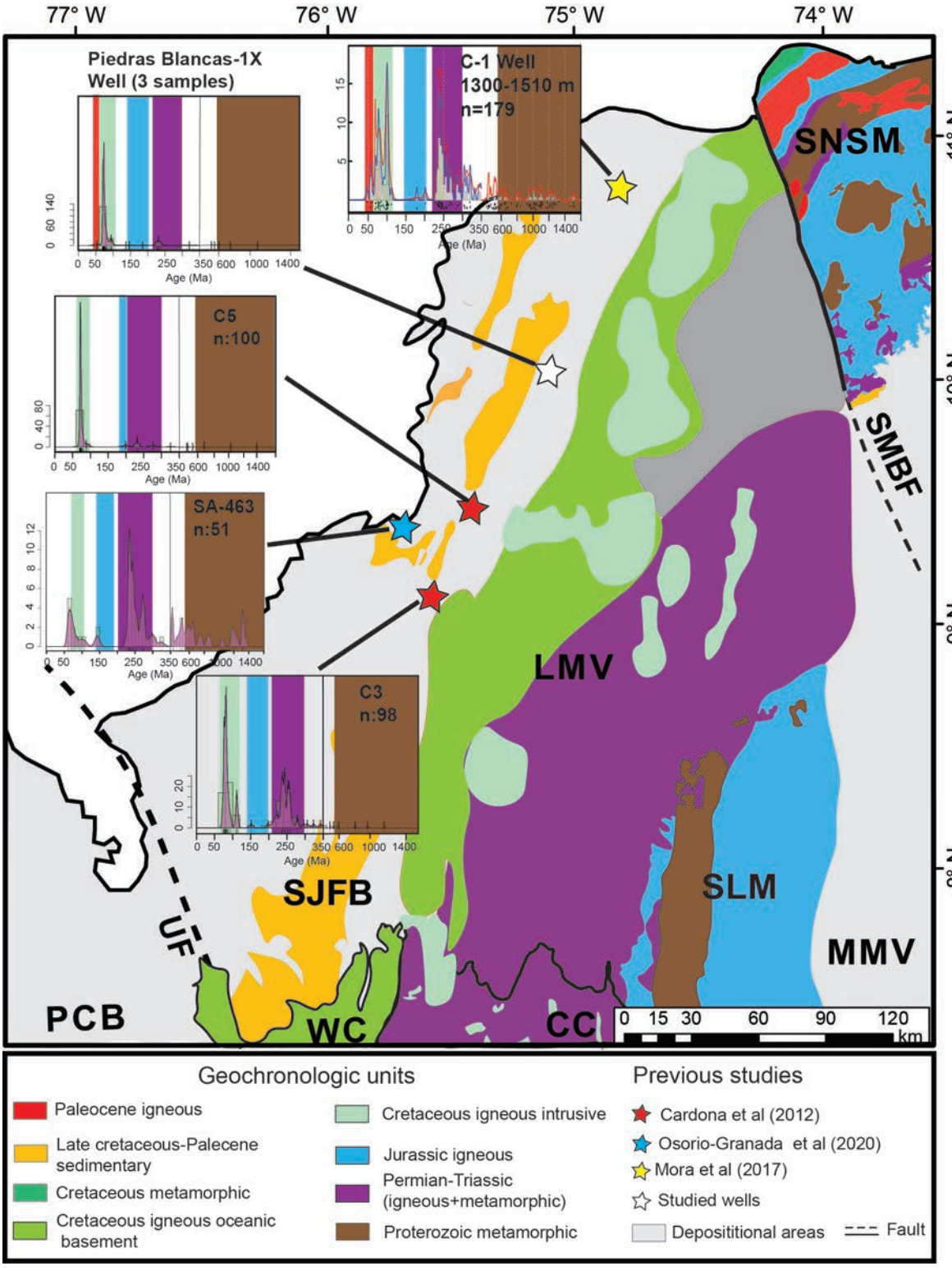

Figure 10. Main chronostratigraphic units in the northern Andes of Colombia considered as potential source areas for Lower Eocene rocks from the San Jacinto Fold Belt (SJFB) and detrital zircons density probability plots for outcrops and wells reported in previous and this study for the Lower Eocene in the studied region. Note that colors in density probability plots match colors of potential source chronostratigraphic units. UF: Uramita fault; SLM: San Lucas Massif; SMBF: Santa Marta-Bucaramanga fault; SFB: Sinú fold belt; LMV: Lower Magdalena Valley; MMV: Middle Magdalena Valley; SNSM: Sierra Nevada de Santa Marta; WC: Western Cordillera; CC: Central Cordillera.

Paleogeographic and magmatic implications

Based on the average petrographic compositions for each studied well and geochronologic results reported in this paper and the integration of provenance data, LMV basement and regional geological information available for the Lower Eocene strata (Montes *et al*., 2010; Cardona *et al*., 2012; Silva-Arias *et al*., 2016; Mora *et al*., 2017; Mora-Bohórquez *et al*., 2017; Osorio-Granada *et al*., 2020) some paleogeographic observations are established. Overall, the proportions of QFL seem to be controlled by the depositional paleoenvironment with deeper environments being more quatz-feldsphatic and more compositionally mature (Figures 5, 6 and 7). Under this observation the more compositionally mature Lower Eocene sedimentary rocks are found in the northern part of the SJFB, where deeper paleoenvironments are present (Figure 11). On the other hand, the proportion of types of lithics in a sandstone seems to be controlled to a lesser extent by the paleoenvironment, being the major control the source availability, therefore, the variability in types of lithics proportions provides the most robust petrographic information on provenance (e.g., Garzanti, 2019). In the studied wells and in the ANH-San Antero-1X well (Osorio-Granada *et al*., 2020), three main sources of lithics (igneous, metamorphic and sedimentary) are present with variability in the lithic composition along the basin. The most remarkable feature is the increase in the proportion of metamorphic lithics in the ANH-La X-1A and ANH-San Antero-1X wells southward of the SJFB (Figure 9). This distribution of the lithic fractions seems to be controlled by local differences in the exposed basement, the proximity of the source to the depositional area, and the East-West drainage trend along the LMV, with the exposed metamorphic source closer to the southern wells (Figures 9 and 11). The Cretaceous-Paleocene sedimentary source outcropping currently westward and southward of the studied wells overall tends to decrease its proportion northward, indicating that the massifs yielding the sedimentary lithics were probably located in the CC foothills with a S-N drainage trend. However, small exposed sedimentary areas located westward cannot be ruled out. The igneous lithic fraction is the higher proportion in the four wells, which agrees with the close location of the Cretaceous igneous source in the LMV (Figures 9, 10 and 11). This magmatic source imprinted the Cretaceous-Paleocene dominant U-Pb peak found in the Lower Eocene wells and outcrops in the SJFB (Figure 10). Another magmatic source in the region is the Triassic felsic granitoids of the LMV basement (Montes *et al*., 2010; Silva-Arias *et al*., 2016; Mora-Bohórquez *et al*., 2017), which are also present in the four wells as suggested by the Permian-Triassic U-Pb peak in the Lower Eocene wells and outcrops (Figure 10).

In addition, the presence of Eocene zircons in the Piedras Blancas-1X well and the Lower Eocene strata of the C-1 well (Mora-Bohórquez *et al*., 2017) may indicate that Eocene magmatism was active during the sedimentation of the SJFB (e.g. Sarmiento *et al*., 2016). Eocene magmatism has been reported in the CC (Leal-Mejía, 2011; Bustamante *et al*., 2017; Rueda-Gutiérrez, 2019), Sierra Nevada de Santa Marta (SNSM), and Guajira (Cardona *et al*., 2010b, 2014), however, the presence of Eocene zircons only in the northern part of the basin (Piedras Blancas-1X and C-1 wells) (Figure 10), the short transport experienced by the studied sediments, and the absence of Eocene metamorphic rocks around the region may indicate that he SNSM is the main source of sediments for the Eocene zircons, but the existence of Eocene igneous rocks in the northern part of the basement of the LMV or SJFB not yet reported is not excluded (Figure 11). If Eocene magmatism was present in the LMV or SJFB then a Late Cretaceous-Paleogene magmatic arc existed along the northern Andes continental margin from the CC to Guajira, probably related to the subduction of the Caribbean plate (e.g., Bayona *et al*., 2012; Mora *et al*., 2018; González *et al*., 2023) (Figure 11D). Under this scenario the Eocene infill of the SJFB was developed as a forearc basin, as suggested by previous studies (e.g., Mora-Bohórquez *et al*., 2020).

The above observations allow us to propose a Lower Eocene paleogeographic model. The paleoenvironments in the studied wells indicate that the southern part of the SJFB was dominated by shallower marine fan delta deposits, while paleoenvironments northward were dominated by deeper submarine fan deposits (ANH-Universidad de Caldas, 2023; Figure 11). Fan delta and submarine fan delta deposits were sourced by nearby sedimentary, igneous and metamorphic rocks associated with the LMV basement, the SJFB itself, and a minor input from distant Jurassic and Proterozoic sources from the San Lucas Massif and/or SNSM. Lithic compositional variability indicates that metamorphic and sedimentary rocks were sourced from south and east and deposited along the SJFB, whereas igneous lithics were sourced by short distance drainage networks and longer drainages from the interior part of the LMV (Figure 11).

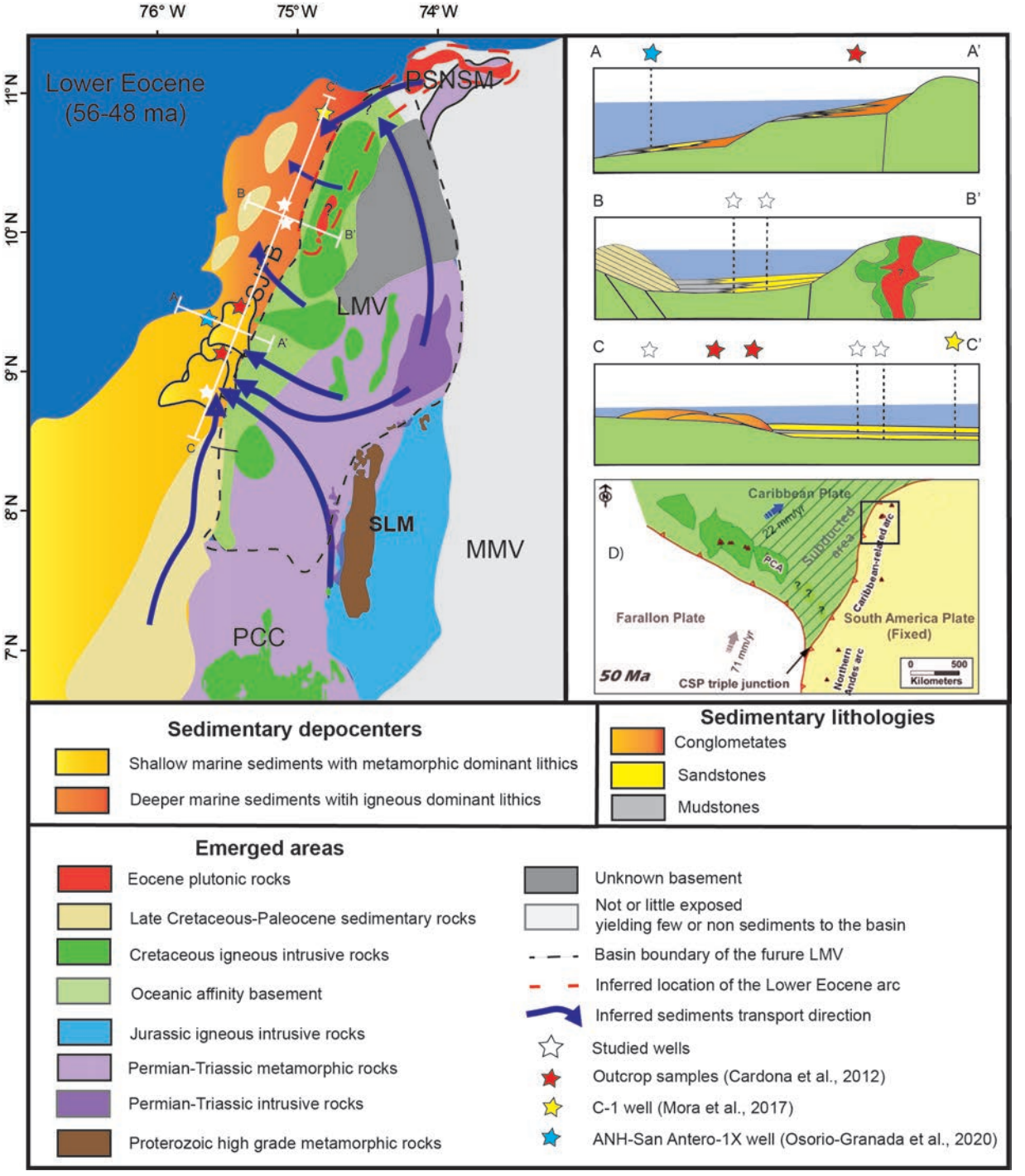

Figure 11. Lower Eocene (56-48 Ma) paleogeographic reconstruction of the SJFB. LMV: Lower Magdalena Valley, PSNSM: Paleo Sierra Nevada de Santa Marta, PCC: Paleo Central Cordillera, MMB: Middle Magdalena Valley, SLM: Paleo San Lucas Massif. **A.-C.** cross sections along the studied region. **D.** Paleo-tectonic reconstruction of the southwestern Caribbean plate motion during the Lower Eocene, showing the migration and convergence of the Panamá-Chocó arc (PCA) against South America, after González *et al*. (2023). CSP: Caribbean-South America-Pacific plates triple junction. The location of the studied area is shown as a black rectangle.

Conclusions

The provenance study of the Lower Eocene sequences in the SJFB documents the presence of several sources of sediments composed of arc-like igneous rocks, metamorphic massifs, and sedimentary rocks. These sources can be associated with proximal LMV basement compositions exposed during the Eocene and currently buried beneath the Oligocene-Pleistocene sedimentary cover. Eocene zircons found in the studied sedimentary rocks suggest that arc magmatism was active during this time, migrating from proximal sources probably located at the SNSM and/or LMV basement. If Eocene magmatic sources originated in the LMV, then a magmatic arc extended along the northern Andes during the Paleogene from the Antioquian Batholith in the Central Cordillera to the Guajira area in the Caribbean, where Paleogene magmatism has been reported. The proposed paleogeographic model suggests that northward sandstones associated with deeper paleoenvironments are more compositionally mature than their southern counterpart.

Acknowledgements

This research is part of the postdoctoral position of Angel Barbosa founded by the Contract 494-2017 in the name of the Special Cooperation Agreement 730/327-2016 signed between the National Hydrocarbons Agency-ANH, the Fondo Nacional para el Financiamiento de la Ciencia, la Tecnología y la Innovación "Fondo Francisco José de Caldas", the Ministerio de Ciencia, Tecnología e Innovación-Minciencias and the Universidad de Caldas. Special thanks are given to The Universidad Nacional de Colombia Sede de La Paz, and to Fabian Gallego and Valentina Vargas for their technical and administrative support. George Kamenov is acknowledged for his help with the U-Pb data acquisition. The staff of the Instituto de Investigaciones en Estratigrafía, Universidad de Caldas is deeply acknowledged for providing important logistic support.

References

Abreu, A. (2009). Determinación del área de aporte de la formación Pendales, cuenca Sinú-San Jacinto, mediante geocronología U-Pb de circones detríticos: un aporte a la evolución tectónica del noroccidente colombiano. Undergraduate thesis, Universidad Nacional de Colombia, Colombia.

Angulo-Pardo, E.; Vallejo-Hincapié, F.; Do Monte-Guerra, R.; Pardo-Trujillo, A.; Giraldo-Villegas, C.A.; García-González, J.; Hernández-Duran, S.; Herrera-Quijano, S.; Plata-Torres, A.; Trejos-Tamayo, R. (2023). Late Cretaceous calcareous nannofossil assemblages from Colombia: Biostratigraphic contributions to northwestern South American Basins. *Journal of South American Earth Sciences, 127*, 104315. https://doi.org/10.1016/j.jsames.2023.104315

ANH-Universidad de Caldas (2009). Estudio integrado de los núcleos y registros obtenidos de 617 los pozos someros tipo "Slim holes" en la Cuenca del Sinú. Informe Final.

ANH-Universidad de Caldas (2023). Certificación de estratigrafía física y de edad de los núcleos de perforación recuperados por la Agencia Nacional de Hidrocarburos–ANH en las cuencas de Sinú–San Jacinto y cordillera. Integración bioestratigráfica. Informe.

Ardila, L.E.; Diaz, L. (2015). Terrane Accretion and Transpression Created New Exploration Frontiers in Northwestern South America. In: C. Bartolini, P. Mann (eds.). *Petroleum geology and potential of the Colombian Caribbean Margin* (pp. 217-245). AAPG. https://doi.org/10.1306/13531938M1083643

Barbosa-Espitia, Á.A.; Kamenov, G.D.; Foster, D.A.; Restrepo-Moreno, S.A.; Pardo-Trujillo, A. (2019). Contemporaneous Paleogene arc-magmatism within continental and accreted oceanic arc complexes in the northwestern Andes and Panama. *Lithos, 348-349*, 105185. https://doi.org/10.1016/j.lithos.2019.105185

Barrero, D.; Pardo, A.; Vargas, C.A.; Martínez, J.F. (2007). *Colombian sedimentary basins: Nomenclature, boundaries and petroleum geology, a new proposal*. Agencia Nacional de Hidrocarburos.

Bayona, G.; Cardona, A.; Jaramillo, C.; Mora, A.; Montes, C.; Valencia, V.; Ayala, C.; Montenegro, O.; Ibañez-Mejia, M. (2012). Early Paleogene magmatism in the northern Andes: Insights on the effects of Oceanic Plateau–continent convergence. *Earth Planetary Science Letters, 331-332*, 97-111. https://doi.org/10.1016/j.epsl.2012.03.015

Bustamante, C.; Cardona, A.; Archanjo, C.J.; Bayona, G.; Lara, M.; Valencia, V. (2017). Geochemistry

and isotopic signatures of Paleogene plutonic and detrital rocks of the Northern Andes of Colombia: A record of post-collisional arc magmatism. *Lithos, 277*, 199-209. https://doi.org/10.1016/j.lithos.2016.11.025

Camargo, G. (1995). Algunos rasgos estructurales del Cinturón del Sinú. *VI Congreso Colombiano del Petróleo*, Bogotá, Colombia.

Cardona, A.; Chew, D.; Valencia, V.A.; Bayona, G.; Mišković, A.; Ibañez-Mejía, M. (2010a). Grenvillian remnants in the Northern Andes: Rodinian and Phanerozoic paleogeographic perspectives. *Journal of South American Earth Sciences, 29*(1), 92-104. https://doi.org/10.1016/j.jsames.2009.07.011

Cardona, A.; Valencia, V.; Bustamante, C.; García-Casco, A.; Ojeda, G.; Ruiz, J.; Saldarriaga, M.; Weber, M. (2010b). Tectonomagmatic setting and provenance of the Santa Marta Schists, northern Colombia: Insights on the growth and approach of Cretaceous Caribbean oceanic terranes to the South American continent. *Journal of South American Earth Sciences, 29*(4), 784-804. https://doi.org/10.1016/j.jsames.2009.08.012

Cardona, A.; Valencia, V.A.; Bayona, G.; Duque, J.; Ducea, M.; Gehrels, G.; Jaramillo, C.; Montes, C.; Ojeda, G.; Ruiz, J. (2011a). Early-subduction-related orogeny in the northern Andes: Turonian to Eocene magmatic and provenance record in the Santa Marta Massif and Rancheria Basin, northern Colombia. *Terra Nova, 23*, 26-34. https://doi.org/10.1111/j.1365-3121.2010.00979.x

Cardona, A.; Valencia, V.; Weber, M.; Duque, J.; Montes, C.; Ojeda, G.; Reiners, P.; Domanik, K.; Nicolescu, S.; Villagómez, D. (2011b). Transient Cenozoic tectonic stages in the southern margin of the Caribbean plate: U-Th/He thermochronological constraints from Eocene plutonic rocks in the Santa Marta massif and Serranía de Jarara, northern Colombia. *Geologica Acta, 9*(3-4), 445-466. https://doi.org/10.1344/105.000001739

Cardona, A.; Montes, C.; Ayala, C.; Bustamante, C.; Hoyos, N.; Montenegro, O.; Ojeda, C.; Niño, H.; Ramirez, V.; Valencia, V.; Rincón, D.; Vervoort, J.; Zapata, S. (2012). From arc-continent collision to continuous convergence, clues from Paleogene conglomerates along the southern Caribbean–South America plate boundary. *Tectonophysics, 580*, 58-87. https://doi.org/10.1016/j.tecto.2012.08.039

Cardona, A.; Weber, M.; Valencia, V.; Bustamante, C.; Montes, C.; Cordani, U.; Muñoz, C. (2014). Geochronology and geochemistry of the Parashi granitoid, NE Colombia: Tectonic implication of short-lived Early Eocene plutonism along the SE Caribbean margin. *Journal of South American Earth Sciences, 50*, 75-92. https://doi.org/10.1016/j.jsames.2013.12.006

Cardona, A.; León, S.; Jaramillo, J.S.; Montes, C.; Valencia, V.; Vanegas, J.; Bustamante, C.; Echeverri, S. (2018). The Paleogene arcs of the northern Andes of Colombia and Panama: Insights on plate kinematic implications from new and existing geochemical, geochronological and isotopic data. *Tectonophysics, 749*, 88-103. https://doi.org/10.1016/j.tecto.2018.10.032

Cediel, F.; Shaw, R.P.; Cáceres, C. (2003). Tectonic assembly of the Northern Andean Block. In: C. Bartolini, R.T. Buffler, J. Blickwede (eds.). *The Circum-Gulf of Mexico and the Caribbean: Hydrocarbon habitats, basin formation, and plate tectonics* (pp. 815-848). AAPG Memoir 79. https://doi.org/10.1306/M79877C37

Cochrane, R.; Spikings, R.; Gerdes, A.; Winkler, W.; Ulianov, A.; Mora, A.; Chiaradia, M. (2014). Distinguishing between in-situ and accretionary growth of continents along active margins. *Lithos, 202-203*, 382-394. https://doi.org/10.1016/j.lithos.2014.05.031

Dickinson, W.R. (1985). Interpreting provenance relations from detrital modes of sandstones. In: G.G. Zuffa (ed.). *Provenance of Arenites* (pp. 333-361). Springer. https://doi.org/10.1007/978-94-017-2809-6_15

Dueñas-Jiménez, H.; Gómez-González, C. (2013). Bioestratigrafía de la Formación Cansona en la quebrada Peñitas, cinturón de San Jacinto. Implicaciones paleogeográficas. *Revista de la Academia Colombiana de Ciencias Exactas, Físicas y Naturales, 37*(145), 527-539. https://doi.org/10.18257/raccefyn.33

Duque-Caro, H. (1979). Major structural elements and evolution of the northwestern Colombia.

In: J.S. Watkins, L. Montadert, P.W. Dickerson (eds.). *Geological and Geophysical Investigations of Continental Margins* (pp.329-351). AAPG Memories. https://doi.org/10.1306/M29405C22

Duque-Caro, H. (1980). Geotectónica y evolución de la región noroccidental colombiana. *Boletín Geológico, 23*(3), 4-37. https://doi.org/10.32685/0120-1425/bolgeol23.3.1980.257

Flinch, J.F. (2003). Structural evolution of the Sinú-Lower Magdalena area (Northern Colombia). In: C. Bartolini, R.T. Buffler, J. Blickwede (eds.). *The Circum-Gulf of Mexico and the Caribbean: Hydrocarbon Habitats, Basin Formation, and Plate Tectonics* (pp. 776-796). AAPG. https://doi.org/10.1306/M79877C35

Folk, R.L. (1980). *Petrology of sedimentary rocks*. Hemphill publishing company.

Garzanti, E. (2019). Petrographic classification of sand and sandstone. *Earth-Science Reviews, 192*, 545-563. https://doi.org/10.1016/j.earscirev.2018.12.014

Gehrels, G. (2011). Detrital Zircon U-Pb Geochronology: Current Methods and New Opportunities. In: C. Busby, A. Azor (eds.). *Tectonics of Sedimentary Basins: Recent advances* (pp. 45-62). John Wiley & Sons. https://doi.org/10.1002/9781444347166.ch2

Gómez, J.; Montes, N.; Marín, E. (2023). Mapa Geológico de Colombia 2023 Escala 1: 1 500 000. Servicio Geológico Colombiano.

González, R.; Oncken, O.; Faccenna, C.; Le Breton, E.; Bezada, M.; Mora, A. (2023). Kinematics and Convergent Tectonics of the Northwestern South American Plate During the Cenozoic. *Geochemistry, Geophysics, Geosystems*, *24*(7), e2022GC010827. https://doi.org/10.1029/2022GC010827

Guzmán, G. (2007). Stratigraphy and sedimentary environment and implications in the Plato Basin and San Jacinto Belt Northwestern Colombia. PhD dissertation. Universidad de Liege, Belgium.

Guzmán, G.; Gómez-Londoño, E.; Serrano-Suárez, B. (2004). Geología de los cinturones del Sinú, San Jacinto y borde occidental del Valle Inferior del Magdalena, Caribe colombiano. INGEOMINAS, Bogotá.

Ibañez-Mejía, M.; Vinasco, C.; Cardona, A.; Valencia, V.; Weber, M. (2010). Permian–Triassic orogenesis in the northern Andes: a record of arc magmatism, accretion, anatexis and relaxation of a continental terrane in the Proto-Andes in the wake of Pangea. *GSA Annual Meeting.* Denver, USA.

Ingersoll, R.V.; Bullard, T.F.; Ford, R.L.; Grimm, J.P.; Pickle, J.D.; Sares, S.W. (1984). The effect of grain size on detrital modes: a test of the Gazzi-Dickinson point-counting method. *Journal of Sedimentary Petrology, 54*(1), 103-116. https://doi.org/10.1306/212F83B9-2B24-11D7-8648000102C1865D

Kennan, L.; Pindell, J.L. (2009). Dextral shear, terrane accretion and basin formation in the Northern Andes: best explained by interaction with a Pacific-derived Caribbean Plate? *Geological Society, London, Special Publications, 328*, 487-531. https://doi.org/10.1144/sp328.20

Košler, J.; Sylvester, P.J. (2003). Present Trends and the Future of Zircon in Geochronology: Laser Ablation ICPMS. *Reviews in Mineralogy and Geochemistry, 53*(1), 243-275. https://doi.org/10.2113/0530243

Leal-Mejía, H. (2011). Phanerozoic Gold Metallogeny in the Colombian Andes: A tectono magmatic approach. Doctoral dissertation, Universitat de Barcelona, Barcelona.

Martini, E. (1971). Standard Tertiary and Quaternary calcareous nannoplankton zonation. *2nd International Conference Planktonic Microfossils*, Roma.

Montes, C.; Guzmán, G.; Bayona, G.; Cardona, A.; Valencia, V.; Jaramillo, C. (2010). Clockwise rotation of the Santa Marta massif and simultaneous Paleogene to Neogene deformation of the Plato-San Jorge and Cesar-Ranchería basins. *Journal of South American Earth Sciences, 29*(4), 832-848. https://doi.org/10.1016/j.jsames.2009.07.010

Mora-Bohórquez, J.A.; Ibánez-Mejia, M.; Oncken, O.; de Freitas, M.; Vélez, V.; Mesa, A.; Serna, L. (2017). Structure and age of the Lower Magdalena Valley basin basement, northern Colombia: New reflection-seismic and U-Pb-Hf insights into the termination of the central Andes against the Caribbean basin. *Journal of South American Earth Sciences, 74*, 1-26. https://doi.org/10.1016/j.jsames.2017.01.001

Mora-Bohórquez, J.A.; Oncken, O.; Le Breton, E.; Ibañez-Mejia, M.; Veloza, G.; Mora, A.; Vélez, V.; De Freitas, M. (2020). Formation and Evolution of the Lower Magdalena Valley Basin and San Jacinto Fold Belt of Northwestern Colombia: Insights from Upper Cretaceous to Recent tectono-stratigraphy. In: J. Gómez, D. Mateus-Zabala (eds.). *The Geology of Colombia* (pp. 21-66). Vol. 3, chapter 2. Servicio Geológico Colombiano. https://doi.org/10.32685/pub.esp.37.2019.02

Mora-Bohórquez, J.A.; Moreno, F.; Ibáñez, M.; Santamaría, L.; Ramírez, R.; Barbosa, J.C.; Góngora, J.D.; Sierra, D.; Veloza, G. (2025). Dating the Chengue/Arroyo de Piedra formation of the northern San Jacinto foldbelt: Results of the application of *in situ* U-Pb carbonate geochronology in NW Colombia. *Journal of South American Earth Sciences*, *153*, 105355. https://doi.org/10.1016/j.jsames.2025.105355

Mora, J.A.; Oncken, O.; Le Breton, E.; Ibánez-Mejia, M.; Faccenna, C.; Veloza, G.; Vélez, V.; de Freitas, M.; Mesa, A. (2017). Linking Late Cretaceous to Eocene Tectono-stratigraphy of the San Jacinto fold belt of NW Colombia with Caribbean plateau collision and flat subduction. *Tectonics*, *36*(11), 2599-2629. https://doi.org/10.1002/2017TC004612

Mora, J.A.; Oncken, O.; Le Breton, E.; Mora, A.; Veloza, G.; Vélez, V.; de Freitas, M. (2018). Controls on forearc basin formation and evolution: Insights from Oligocene to Recent tectono-stratigraphy of the Lower Magdalena Valley basin of northwest Colombia. *Marine and Petroleum Geology, 97*, 288-310. https://doi.org/10.1016/j.marpetgeo.2018.06.032

Ordóñez-Carmona, O.; Frantz, J.; Chemale, F.; Londoño, C. (2009). Serranía de San Lucas: mineralizaciones auríferas, intrusiones de 1500 Ma, metamorfismo Grenville y magmatismo Jurásico. *XII Congreso Colombiano de Geología*. Paipa, Colombia. https://doi.org/10.13140/2.1.2705.1525

Osorio-Granada, E.; Pardo-Trujillo, A.; Restrepo-Moreno, S.A.; Gallego, F.; Muñoz, J.; Plata, A.; Trejos-Tamayo, R.; Vallejo, F.; Barbosa-Espitia, A.; Cardona-Sánchez, F.J.; Foster, D.A.; Kamenov, G. (2020). Provenance of Eocene–Oligocene sediments in the San Jacinto Fold Belt: Paleogeographic and geodynamic implications for the northern Andes and the southern Caribbean. *Geosphere, 16*(1), 210-228. https://doi.org/10.1130/GES02059.1

Parra, M.; Echeverri, S.; Patiño, A.M.; Ramirez, J.C.; Mora, A.; Sobel, E.R.; Almendral, A.; Pardo-Trujillo, A. (2020). Cenozoic Evolution of the Sierra Nevada de Santa Marta, Colombia. In: J. Gómez, D. Mateus-Zabala (eds.). *The Geology of Colombia* (pp. 185-13). Vol. 3, chapter 7. Servicio Geológico Colombiano. https://doi.org/10.32685/pub.esp.37.2019.07

Patarroyo, G.D.; Plata, J.S.; Suárez, S.A.; Torres, G.A.; Veloza, G.; Mora-Bohórquez, J.A.; Gómez, D.F.; Torres, J.M. (2025). Caracterización litológica y bioestratigráfica de la Formación Toluviejo: aportes a la reconstrucción paleoambiental de las sucesiones carbonáticas del Eoceno en el norte de Colombia. *Boletín de Geología, 47*(1), 43-61. https://doi.org/10.18273/revbol.v47n1-2025002

Pindell, J.L.; Kennan, L. (2009). Tectonic evolution of the Gulf of Mexico, Caribbean and northern South America in the mantle reference frame: an update. *Geological Society, London, Special Publications, 328*, 1-55. https://doi.org/10.1144/SP328.1

Piraquive, A.; Kammer, A.; Bernet, M.; Cramer, T.; von Quadt, A.; Gómez, C. (2022). Neoproterozoic to Jurassic tectono-metamorphic events in the Sierra Nevada de Santa Marta Massif, Colombia: insights from zircon U-Pb geochronology and trace element geochemistry. *International Geology Review, 64*(14), 1933-1965. https://doi.org/10.1080/00206814.2021.1961317

Plata-Torres, A.; Pardo-Trujillo, A.; Vallejo-Hincapié, F.; Trejos-Tamayo, R.; Flores, J.A. (2023). Early Eocene (Ypresian) palynology of marine sediments from the colombian Caribbean. *Journal of South American Earth Sciences, 121*, 104146. https://doi.org/10.1016/j.jsames.2022.104146

Restrepo-Moreno, S.A.; Foster, D.A.; Stockli, D.F.; Parra-Sánchez, L.N. (2009). Long-term erosion and exhumation of the "Altiplano Antioqueño", Northern Andes (Colombia) from apatite (U-Th)/He thermochronology. *Earth and Planetary Science Letters, 278*(1-2), 1-12. https://doi.org/10.1016/j.epsl.2008.09.037

Reyes, G.; Camargo, G. (1995). Esquema estructural del Cinturón de San Jacinto. *VI Congreso Colombiano del Petróleo*, Bogotá, Colombia.

Rueda-Gutiérrez, J.B. (2019). Aportes al conocimiento del Magmatismo de la Cordillera Central de Colombia en su Flanco Oriental: Área geotérmica de San Diego, Samaná, Caldas. *Boletín de Geología, 41*(2), 45-70. https://doi.org/10.18273/revbol.v41n2-2019003

Sarmiento, G.; Bonilla, G.; Osorio, J. (2016). Evidencias de Vulcanismo Penecontemporáneo en la Formación San Cayetano de la Cuenca Sinu-San Jacinto e Implicaciones en el entorno geológico regional. *The Colombian and Venezuelan Caribbean Geology Workshop*, Bogotá.

Sierra, D.; Mora, J.A.; Veloza, G.; Ruiz, J.C.; Fechi, Y. (2024). Evolución geológica del Eoceno Medio al Reciente en el extremo norte del Cinturón Plegado de San Jacinto. *1ra Convención de Exploración Energética*, Santa Marta, Colombia.

Silva-Arias, A.; Páez-Acuña, L.A.; Rincón-Martínez, D.; Tamara-Guevara, J.A.; Gomez-Gutierrez, P.D.; López-Ramos, E.; Restrepo-Acevedo, S.M.; Mantilla-Figueroa, L.C.; Valencia, V. (2016). Basement characteristics in the Lower Magdalena Valley and the Sinú and San Jacinto Fold Belts: Evidence of a Late Cretaceous Magmatic Arc at the South of the Colombian Caribbean. *CT&F - Ciencia, Tecnología y Futuro, 6*(4), 5-36. https://doi.org/10.29047/01225383.01

Suttner, L.J.; Dutta, P.K. (1986). Alluvial sandstone composition and paleoclimate; I, Framework mineralogy. *Journal of Sedimentary Petrology, 56*(3), 329-345. https://doi.org/10.1306/212F8909-2B24-11D7-8648000102C1865D

Taylor, A.M.; Goldring, R. (1993). Description and analysis of bioturbation and ichnofabric. *Journal of the Geological Society, 150*(1), 141-148. https://doi.org/10.1144/gsjgs.150.1.0141

Vallejo-Hincapié, D.F.; Aubry, M.P.; Pardo-Trujillo, A.; Trejos-Tamayo, R.; Plata, A.; Salazar-Ríos, A.; Diaz-Jaramillo, A.; Osorio, J.A. (2019). Early Eocene (Ypresian) calcareous nannofossil stratigraphy from the Caribbean region of Colombia, South America. In: R.A. Denne, A. Kahn (eds.). *Geologic problem solving with microfossils IV* (pp. 161-171). Vol. 111. Society for Sedimentary Geology. https://doi.org/10.2110/sepmsp.111.07

Vallejo-Hincapié, F.; Flores, J.A.; Marie-Pierre, A.; Pardo-Trujillo, A. (2023). Contribution to the Cenozoic chronostratigraphic framework of the Caribbean Sinú-San Jacinto Belt of Colombia based on calcareous nannofossils. *Journal of South American Earth Sciences, 127*, 104419. https://doi.org/10.1016/j.jsames.2023.104419

Villagómez, D.; Spikings, R.; Magna, T.; Kammer, A.; Winkler, W.; Beltrán, A. (2011a). Geochronology, geochemistry and tectonic evolution of the Western and Central cordilleras of Colombia. *Lithos, 125*(3-4), 875-896. https://doi.org/10.1016/j.lithos.2011.05.003

Villagómez, D.; Spikings, R.; Mora, A.; Guzmán, G.; Ojeda, G.; Cortés, E.; van der Lelij, R. (2011b). Vertical tectonics at a continental crust-oceanic plateau plate boundary zone: Fission track thermochronology of the Sierra Nevada de Santa Marta, Colombia. *Tectonics, 30*(4). https://doi.org/10.1029/2010TC002835

Villagómez, D.; Spikings, R. (2013). Thermochronology and tectonics of the Central and Western Cordilleras of Colombia: Early Cretaceous–Tertiary evolution of the northern Andes. *Lithos, 160-161*, 228-249. https://doi.org/10.1016/j.lithos.2012.12.008

Vinasco, C.J.; Cordani, U.G.; González, H.; Weber, M.; Pelaez, C. (2006). Geochronological, isotopic, and geochemical data from Permo-Triassic granitic gneisses and granitoids of the Colombian Central Andes. *Journal of South American Earth Sciences, 21*(4), 355-371. https://doi.org/10.1016/j.jsames.2006.07.007

Received: 21 August 2024
Accepted: 23 May 2025